



HYD-RESPONSES: daily hydro-meteorological catchment-level time series to analyse HYDrological drought dynamics in RESPONSE to (cumulative) water deficits in Swiss catchments.

Christoph Nathanael von Matt^{1,2}, Benjamin David Stocker^{1,2}, and Olivia Martius^{1,2}

¹Institute of Geography, University of Bern, Bern, Switzerland

²Oeschger Center for Climate Change Research, University of Bern, Bern, Switzerland

Correspondence: Christoph Nathanael von Matt (christoph.vonmatt@unibe.ch)

Abstract.

The HYD-RESPONSES dataset (<https://doi.org/10.5281/zenodo.14713274>; von Matt et al., 2025) provides new daily catchment-level time series for key hydro-meteorological variables necessary to study drought conditions, including precipitation, snow water equivalent, temperature, soil moisture, (potential) evaporation, and streamflow. The dataset covers 184 small to large Swiss catchments of the surface water monitoring network operated by the Federal Office for the Environment (FOEN). The catchments range across a variety of streamflow regime types, mean altitudes, biogeographic regions, and anthropogenic influences. The data set provides daily average streamflow derived from measurements by the FOEN and daily hydrometeorological data (precipitation, temperature, radiation, snow and soil moisture) on the catchment level extracted from spatially gridded data provided by MeteoSwiss (RhiresD, TabsD, TmaxD, TminD, SrelD), MeteoSwiss and the WSL Institute for Snow and Avalanche Research SLF (SPASS), SLF (OSHD), and the European Centre for Medium-Range Weather Forecasts ECMWF (ERA5-Land).

In addition, derived indicators describing snowfall, snowmelt, (potential) water balance and streamflow are provided. Information on precipitation, evaporation-driven and streamflow deficits are provided in form of standardized and non-standardized (drought/deficit) indices. Standardized indices include the SPI, SPEI and SMRI and are provided on multiple aggregation scales from 1 to 24 months (mostly in 3-monthly steps). Non-standardized indices are provided as cumulative (water) deficits in (potential) water balance (CWD and PCWD) and streamflow (CQD). For all variables and indices, the climatology and the (standardized) anomalies are available on various time scales (daily, monthly, seasonal, and yearly). Drought event time series containing drought event numbers and drought event durations, are provided for streamflow droughts identified by using two percentile-based event definitions (fixed and variable threshold) and for cumulative water deficits (CWD, PCWD and CQD).

Detailed catchment descriptors covering hydro-climatological and hydro-terrestrial aspects as well as streamflow characteristics are provided for all catchments. The dataset can be used to study weather-driven streamflow extremes, to train data-driven machine-learning algorithms, to study drought propagation, and for comparative analyses of catchment responses in disturbed and undisturbed catchments. The dataset is compatible with the recently published CAMELS-CH dataset and with additional catchment descriptors provided by the FOEN.



1 Introduction

In recent years, the frequency of droughts has increased in Europe and Switzerland with notable drought years in 2003, 2011, 2015, 2018, 2020. Most recently, in 2022, conditions were characterized as unprecedented in terms of compound heat and drought in the last 500 years over large parts of Europe (BAFU, 2016; BAFU et al. (Hrsg.), 2019; BUWAL, BWG, MeteoSchweiz, 2004; Scherrer et al., 2022; Tripathy and Mishra, 2023). Under climate change, this trend is likely to continue with projected increases in drought frequency, dry spell duration, and drought severity for both individual and combined drought types (Brunner et al., 2019b, a; Calanca, 2007; Kotlarski et al., 2023; Muelchi et al., 2021a; von Matt et al., 2024). Increasing drought impacts on various sectors are expected. This has prompted Swiss national authorities to establish a national drought early warning system (DEWS, see <https://www.trockenheit.admin.ch/en>; BAFU (Hrsg.), 2021; CH2018, 2018; Haile et al., 2020; Henne et al., 2018; Naumann et al., 2021; Brunner et al., 2019a; Otero et al., 2023; Ranasinghe et al., 2021; Tschurr et al., 2020; BAFU, 2022; Swiss Confederation, 2025).

Droughts are an inherently multivariate phenomenon with often non-linear drought propagation from meteorological conditions to impacts on ecosystems, infrastructure, and economy. Individual drought events may differ in their hydro-climatological, hydro-meteorological, hydro-terrestrial and anthropogenic characteristics (Brunner et al., 2023; Hao and Singh, 2015; Mishra and Singh, 2010; Zhou et al., 2021; Floriancic et al., 2020; Massari et al., 2022). The consideration of multiple hydro-climatic, hydro-meteorological, hydro-terrestrial and anthropogenic factors is therefore key to understand catchment-specific drought responses and sensitivities and to provide information for drought early warning, preparations, and interventions (e.g., Apurv et al., 2017; Apurv and Cai, 2020; Baez-Villanueva et al., 2024; Brunner et al., 2022, 2021; Ding et al., 2021; Peña-Angulo et al., 2022; Peña-Gallardo et al., 2019; Sutanto and Van Lanen, 2022; Tjiedeman et al., 2018; Van Lanen et al., 2013; Savelli et al., 2022; Van Loon and Laaha, 2015; von Matt et al., 2024).

Novel high-resolution observational datasets provide a unique opportunity to combine multiple hydro-meteorological variables to analyze and monitor drought dynamics and the evolution of drought impacts of individual events at the catchment-level. For example, the propagation of meteorological to hydrological droughts or the evolution of droughts from the development to the recovery phase can be studied (Brunner et al., 2021; Brunner and Chartier-Rescan, 2024; Parry et al., 2016; Raposo et al., 2023; Brocca et al., 2024; Brunner et al., 2021; Stocker et al., 2023; Poussin et al., 2021). The Federal Office for Climatology and Meteorology (MeteoSwiss) provides a suite of high-resolution essential climate variables spatially interpolated to a regular grid from a dense measurement station network (MeteoSwiss, 2024). Further, new high-resolution snow climatologies produced by both MeteoSwiss and the WSL Institute for Snow and Avalanche research SLF have recently become available, providing a novel opportunity to analyze the long-term influence of snow processes, which are crucial for streamflow (drought) generation in Alpine catchments in Switzerland (Staudinger et al., 2014, 2017; Avanzi et al., 2024; Brunner et al., 2023; Koehler et al., 2022; Michel et al., 2023; Marty et al., 2025).

Observation-based evapotranspiration and soil moisture data is sparse in Switzerland. Hence, information on these variables is often extracted from hydrological model simulations Brunner et al. (2021); Melsen and Guse (2019); Samaniego et al. (2013, 2018). The ERA5-Land reanalysis dataset, provided by the European Centre for Medium-Range Weather Forecasts



(ECMWF) (Muñoz-Sabater et al., 2021), offers a compromise between high spatial resolution and long temporal coverage and is better suited for hydro-meteorological analyses and modelling over more complex terrain such as Switzerland than the ERA5 reanalysis datasets (Muñoz-Sabater et al., 2021). A frequently used approach for analyzing drought propagation from meteorological (precipitation) to agricultural (soil moisture) and hydrological (streamflow and/or groundwater) droughts relies on standardized drought indices based on e.g., precipitation and/or evaporation (by using the standardized precipitation index (SPI) or the standardized precipitation evaporation index (SPEI) (Raposo et al., 2023; Barker et al., 2016; Peña-Gallardo et al., 2019; Zhou et al., 2021). These standardized drought indices are typically aggregated over varying retrospective time scales (months to years) and are useful proxies for various factors that determine catchment-scale water balances, including soil moisture, streamflow, groundwater, and snow processes (Bachmair et al., 2018; Tschurr et al., 2020; European Commission, 2020; Cammalleri et al., 2019; Staudinger et al., 2014). Longer aggregation scales hereby reflect response scales of storage components with longer memory, while shorter scales reflect streamflow and/or soil moisture in smaller catchments, mainly influenced by pluvial processes (Bachmair et al., 2018; Baez-Villanueva et al., 2024; Haslinger et al., 2014; Myrionidis et al., 2018; Staudinger et al., 2014; Tschurr et al., 2020; WMO and GWP, 2016; Yihdego et al., 2019; Cammalleri et al., 2019; Bachmair et al., 2016; European Commission, 2020). Standardized drought indices are now widely used in DEWS (Bachmair et al., 2016; Kchouk et al., 2022; Raposo et al., 2023; Tjrdeman et al., 2020) and will also be used in the Swiss DEWS (L. Benelli, pers. comm.).

Recent studies focused on assessing the benefits of non-standardized (deficit) indices in tracking the drought propagation signal across drought types (see e.g., Brunner and Chartier-Rescan, 2024; Sur et al., 2020; Wu et al., 2020). Non-standardized indices provide physically interpretable and consistent information on deficits which remain inter-comparable across systems as a result of non-transformation (Van Loon, 2015; Raposo et al., 2023; Wu et al., 2020). Examples are the Hydrological Anomaly Index (HAI), the Water Balance Drought Index (WBDI), the cumulative water deficits (CWD), and the potential cumulative water deficit (PCWD) (Stocker et al., 2023; Sur et al., 2020; Wu et al., 2020). Non-standardized indices allow direct quantification of (precipitation) deficits or surpluses associated with the drought propagation into and recovery from a (hydrological) droughts (Wu et al., 2020) and hence provide valuable information for proactive water management and decision-making (Xu et al., 2023; Parry et al., 2018).

Here, we present a novel dataset with high-resolution observational daily catchment-level time series for key hydro-meteorological variables (including precipitation, snow water equivalent, temperature, soil moisture, (potential) evaporation and streamflow), standardized and non-standardized (drought/deficit) indices (SPI, SPEI, SMRI, CWD, PCWD, CQD) and (streamflow) drought events covering 184 small to large catchments in Switzerland. The HYD-RESPONSES dataset can be combined with existing hydro-meteorological time series datasets and catchment descriptors such as CAMELS-CH (Höge et al., 2023a).

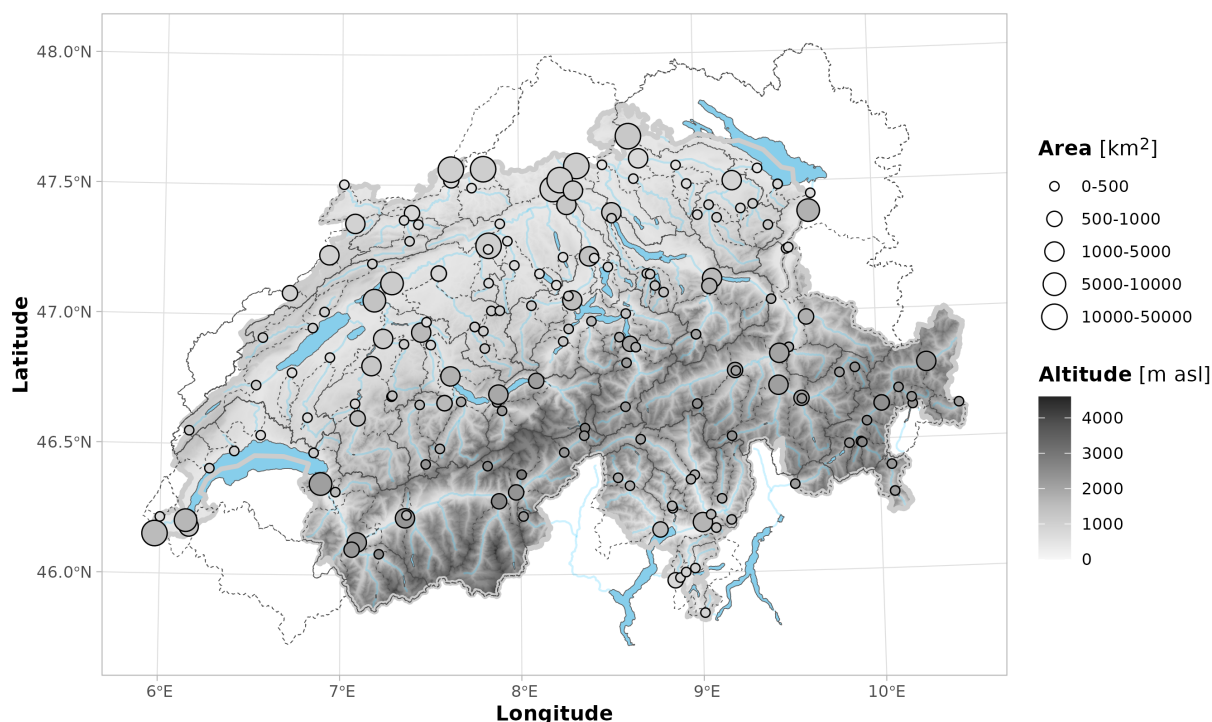


Figure 1. Overview of the study area and catchments included in the HYD-RESPONSES dataset. Catchment outlets (circles) are coloured by mean catchment altitude [m a.s.l.] and the point size scales with the catchment area [km²]. Dashed lines show the catchment outlines. Generalized streamflow networks and lakes are shown in light blue.

2 Study region and catchments

The 184 catchments (Fig. 1) provided in the HYD-RESPONSES dataset span a wide range of catchment areas (0.56–35'878 km²), glaciation percentages (0–56 %), altitude ranges (467–2937 m a.s.l.) and streamflow regime types (n=18) (see Fig. 3). More than half (n=94 (51 %)) of the catchments are small to mid-sized with an area of between 10 km² and 500 km². 9 (4 %)
 95 catchments are smaller than 10 km² and 56 (30.4 %) catchments are larger than 500 km². The dataset contains eight very large catchments with areas between 10000 km² and 50000 km² (max. area = 35'878 km²), associated with the three largest rivers in Switzerland: Aare, Rhine and Rhone. Most catchments (82.5 %) have less than 5 % glaciated area. The catchments are distributed relatively equally between 500 and 2500 m a.s.l. with fewer (77 out of 98) catchments at elevation ranges above 1500 m a.s.l.. Only eight catchments are higher than 2500 m a.s.l. and only one catchment is at very low elevation (catchment
 100 Wiese, Basel). Streamflow regime types were classified and adjusted by the FOEN based on data from the Hydrological Atlas of Switzerland Table 5.2 (https://hydrologischeratlas.ch/downloads/01/content/Tafel_52.pdf). Catchments smaller than 500 km² are characterized by considering mean altitude and catchment glaciation percentage to reflect the contribution of specific streamflow (drought) generating processes (glacial, nival, pluvial). Catchments larger than 500 km² are generally classified



as *mixed regime* ($>500 \text{ km}^2$) type and contain catchments characterized by a combination of streamflow (drought) generating
 105 processes. For more information see also Aschwanden and Weingartner (1985) and Fig. 3e.

3 Input data products

In this section, the input datasets used to produce and compile the HYD-RESPONSES dataset are presented and reference
 literature for further reading and more detailed information is provided. Original data products are provided by the Federal
 Office for Climatology and Meteorology (MeteoSwiss), the Federal Office for the Environment (FOEN), the Swiss Federal
 110 Office of Topography (Swisstopo), the Federal Office for Agriculture (FOAG), the WSL Institute for Snow and Avalanche
 Research (SLF) and the European Centre for Medium-Range Weather Forecasts (ECMWF).

3.1 Catchment-level time series data from streamflow observations

Daily average streamflow measurements at the catchment outlet were provided by the FOEN via the Hydrological Service
 (www.hydrodaten.admin.ch) for more than 200 stations. The data availability is station-specific and depends on the installa-
 115 tion and FOEN-internal data quality checking. The HYD-RESPONSES dataset only provides a subset of 184 catchments by
 considering only stations for which an analysis of hydrological drought dynamics in response to cumulative water deficits was
 deemed to be meaningful in correspondence with the FOEN (Caroline Kan; see Fig. 1). Stations were excluded in case of
 i) Q measured at water-level stations (3 stations), ii) Q measured at NADUF-stations (4 stations), iii) secondary stations (11
 stations), iv) stations with potential return (= negative) streamflow (2 stations), v) Q measured at derivations (2 stations), vi)
 120 stations with no watershed delineation (i.e., subterranean; 1 station) and vii) uncertainties in time series composition due to
 displacement and/or temporarily missing Q of contributing stations (4 stations). A complete list of included stations is provided
 in Tables A2, A3, A4 and A6 (Appendix).

3.2 Catchment-level time series data derived from spatially gridded products

Meteorological variables (except for evaporation) were assembled from the high-resolution ($1 \times 1 \text{ km}$) spatial climate analyses
 125 provided by MeteoSwiss (MeteoSwiss, 2024) (see Table 1). The variables include average 2 m temperature (TabsD), daily
 minimum and maximum 2 m temperature (TminD, TmaxD), daily precipitation sums (RhiresD) and daily sunshine duration
 (SrelD) (Frei, 2014; Frei and Schär, 1998; MeteoSwiss, 2021a, b, c). The data availability is product-specific and covers the
 period 1961–2023 for RhiresD and TabsD and 1971–2023 for the other products (TminD, TmaxD, SrelD). The spatial climate
 analyses products used here only cover the Swiss territory, except for RhiresD, which covers catchments located outside
 130 Switzerland, but draining through Swiss territory. Note that RhiresD is not available for catchments covering regions in France
 and Italy before 1992 due to limited meteorological station availability and hence limited data reliability (MeteoSwiss, 2021a).
 Catchments with a significant area in France or Italy may therefore be handled with care and/or potentially be excluded from
 analysis before 1992 (see Section 7).



Table 1. (Spatially gridded) products used for the time series extraction

Dataset	Variables	Period	Spatial resolution	Temporal resolution	Producer
Spatial Climate Analyses	TabsD, RhiresD	1961–2023	1 × 1 km	daily	MeteoSwiss
	TminD, TmaxD, SrelD	1971–2023			
Snow Climatology for Switzerland (SPASS)	SWECLQMD	1961–2022	1 × 1 km	daily	MeteoSwiss & SLF
Climatological snow data since 1998 (OSHD)	swee, romc	1998–2023	1 × 1 km	daily	SLF
ERA5-Land	tp, t2m, e, pev, smlt, sd, ssr, ro, sro, swvl1, swvl2, swvl3, swvl4	1950–2023	0.1 × 0.1° (ca. 9 × 9 km)	hourly	ECMWF
Streamflow time series	Q	Station specific	catchment-level (outflow point data)	daily	FOEN

135 Snow water equivalent (SWE) data was compiled from two high-resolution (1 × 1 km) datasets. The first and main product resulted from the joint research project “A spatial Snow Climatology for Switzerland (SPASS)” by MeteoSwiss and SLF (Michel et al., 2023; Marty et al., 2025). The preliminary version was produced in 2022 and provides modelled and bias-corrected daily SWE data for the period September 1961–September 2022. The spatial extent is restricted to the Swiss territory. The SPASS SWE is based on the daily TabsD and RhiresD products (see above) and makes use of a quantile-mapping approach. The model is presented in detail in Michel et al. (2023). The second snow product is based on the Swiss Operational Snow-hydrological model system (OSHD) and is provided by the WSL (SLF) (Mott, 2023; Mott et al., 2023). The OSHD data provides information on both SWE and snowmelt runoff for the period 1998–2022 (Mott, 2023; Mott et al., 2023).

145 All other hydro-meteorological variables, including evaporation, potential evaporation, soil moisture and additional variables already covered by the previously introduced datasets, were extracted from the ERA5-Land reanalysis dataset provided by ECMWF (Muñoz-Sabater et al., 2021). Several variables are therefore covered by multiple source data and are all included in the HYD-RESPONSES dataset to allow comparative analyses between the different data products. Time series covered by multiple data sources include temperature variables (TabsD, TminD and TmaxD from MeteoSwiss, t2m from ERA5-Land), precipitation (RhiresD from MeteoSwiss, precipitation from ERA5-Land), potential and total evaporation (ERA5-Land), sunshine duration (SrelD), snow water equivalent (SWE; from SPASS, OSHD, and ERA5-Land), modelled snow melt (from OSHD and ERA5-Land) and streamflow (FOEN). Additional variables extracted from ERA5-Land include four soil water



Table 2. Data products used to extract catchment descriptors.

Dataset	(Extracted) Variables	Producer
Digital soil suitability maps of Switzerland	soil wetness, soil depth, permeability, water holding capacity, nutrient content and skeletal content	FOAG
Hydrogeological map of Switzerland	aquifer type (loose or solid rock), aquifer genesis and aquifer productivity	FOEN
Lithological map for Switzerland	dominant rock type classes (loose, sedimentary and crystalline rock)	Swisstopo
Springs and swallow holes in karst regions	number of springs (per km ²)	FOEN
swissALTI3D (DEM)	aspect, slope	Swisstopo
swissTLM3D Hydrography	Drainage density	Swisstopo
Biogeographic regions of Switzerland	Biogeographic regions	FOEN
Catchment metadata	time series availability, breakpoint analysis, area, mean height, outlet coordinates and streamflow regime type	FOEN

volume levels (swvl), total solar radiation (ssr) and runoff (ro) and surface runoff (sro). For a more detailed description of variables, see the data documentation on Zenodo (von Matt et al., 2025). A glossary of variable abbreviations is provided in Table A1.

155 The ERA5-Land data is provided at an hourly temporal resolution for the period 1950–2023 and can be accessed via the Copernicus climate data store (CDS) (<https://cds.climate.copernicus.eu/datasets/reanalysis-era5-land>). We preferably included data from ERA5-Land over data from ERA5 due to the higher spatial resolution of ERA5-Land ($0.1 \times 0.1^\circ$, ca. 9×9 km). To ensure consistency with the other hydro-meteorological input datasets, the hourly ERA5-Land data was aggregated to daily values (see Section 4.1).

160 3.3 Catchment-level time-invariant data (catchment descriptors)

Datasets used to compile an extensive set of catchment descriptors include station metadata and information on time series availability and homogeneity provided by the FOEN as well as spatial (polygon) data on hydro-terrestrial characteristics (e.g., soil characteristics, hydro-geology) provided by the FOEN, FOAG and Swisstopo (see Tab. 2). Most information is available from www.opendata.swiss, the FOEN Hydro-Service (www.hydrodaten.admin.ch), or can be downloaded and inspected via www.map.geo.admin.ch (Swisstopo). Direct links to the datasets are provided below in section 10.

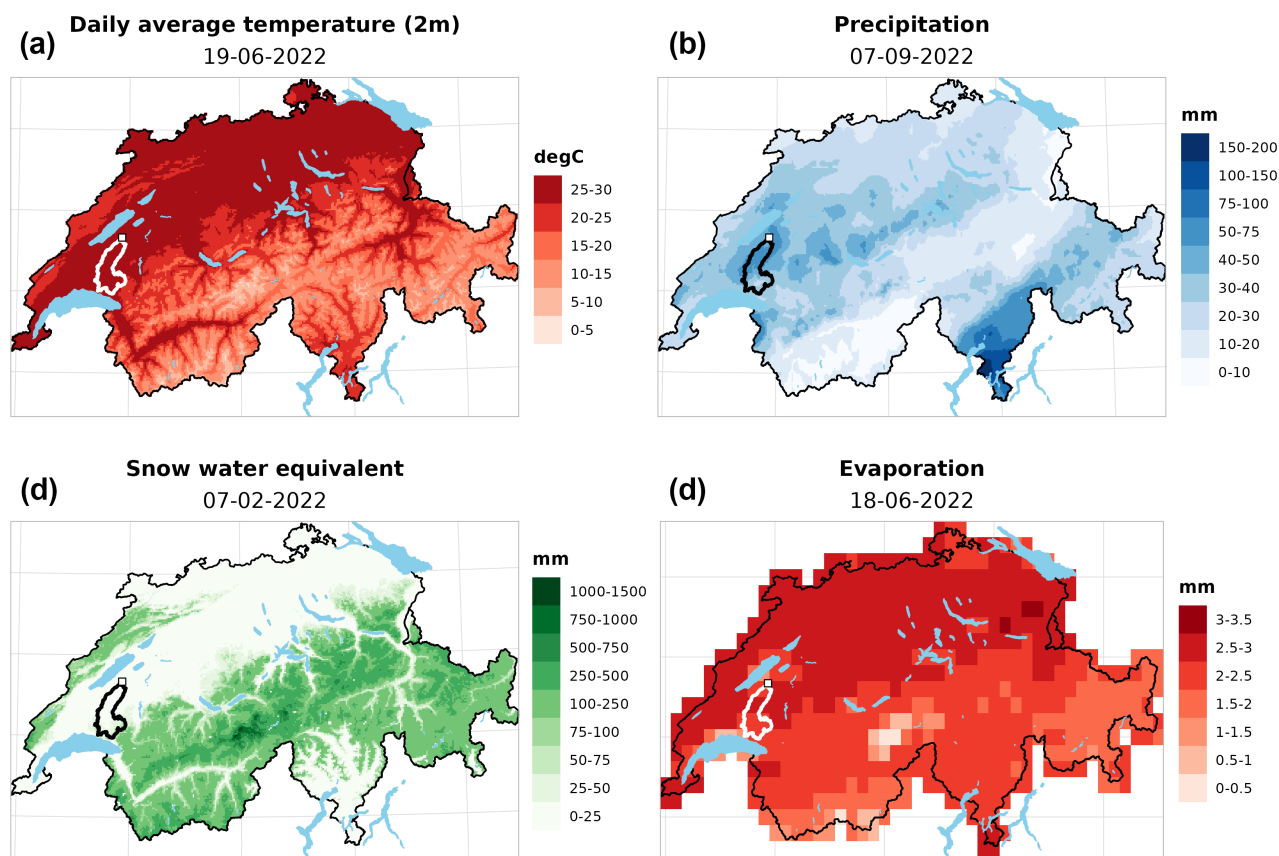


Figure 2. Overview of the spatial raster products used to extract daily time series. (a) Mean daily temperature (TabsD, MeteoSwiss), (b) Daily precipitation sun (RhiresD, MeteoSwiss), (c) Daily snow water equivalent of the Swiss snow climatology (SPASS) (SWE, MeteoSwiss & SLF), (d) Daily evaporation sum (aggregated from hourly ERA5-Land data, ECMWF). Note that the second snow climatology product (OSHD) is not shown. Contours in white/black show catchment 2034 - Broye, Payerne, Casernde d'aviation for the day with the highest observed catchment average values for each specific product for the year 2022. White squares show the catchment outlet where daily streamflow is measured. Extracted and derived time series over the year 2022 are shown for the same catchment in Figure 9.

The digital soil suitability maps provide information on a set of different soil characteristics assessed on 25 different geological and geomorphological units which are further discriminated by different landscape elements depending on aspect, slope and bedrock. The maps were first assessed in 1980 and revised in 2000 (BLW, 2022; Swisstopo, 2020). The different soil characteristics include soil wetness, soil depth, permeability, water storage capacity, nutrient content and skeletal content. The hydro-geological map of Switzerland provides information on groundwater resources in Switzerland (Schürch et al., 2007), including information on aquifer type (loose or solid rock), aquifer genesis and aquifer productivity. The map was originally produced and published for the Hydrological Atlas of Switzerland (HADES, <https://hydrologischeratlas.ch/>). The



Basic catchment characteristics

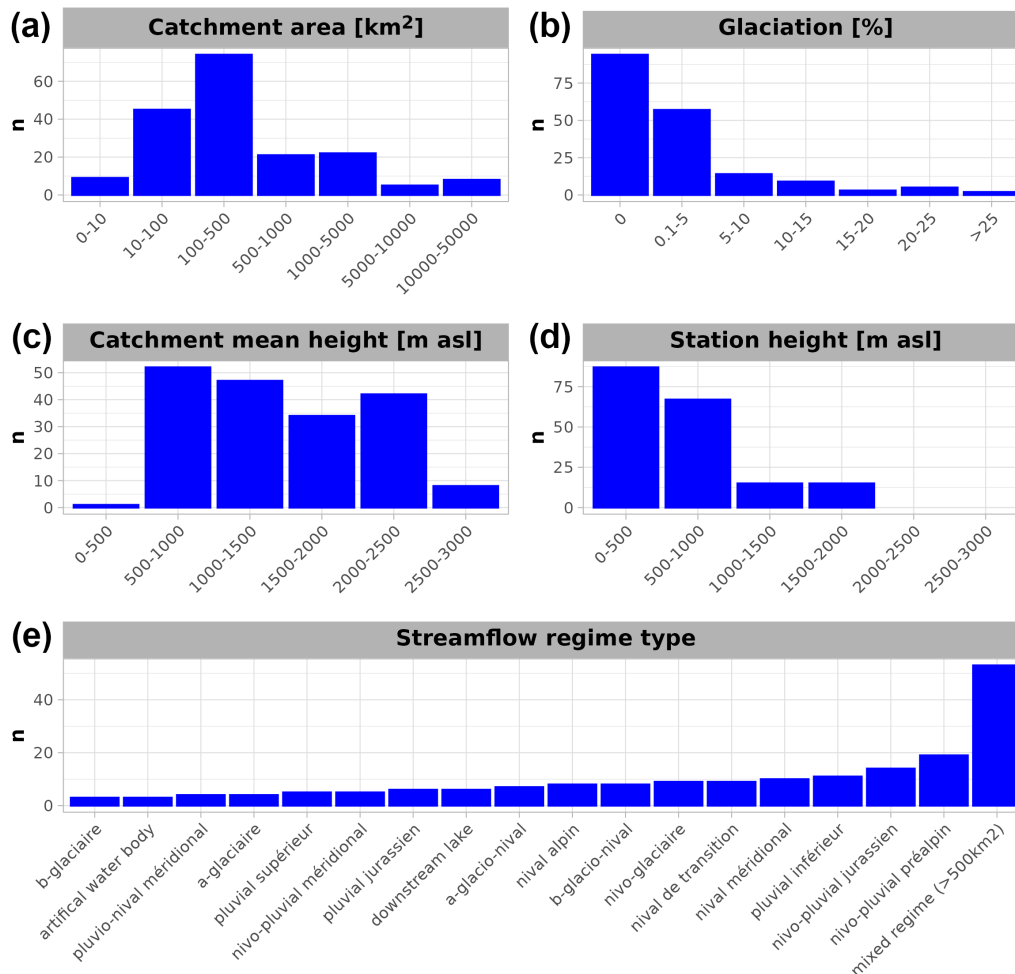


Figure 3. General catchment characteristics provided by the FOEN. **a)** Catchment area in km², **b)** Glaciation percentage (of catchment area), **c)** catchment mean height [m a.s.l.], **d)** height of the streamflow gauge measurement station [m a.s.l.] and **e)** streamflow regime types. The Y-axis shows the frequency of each category.

hydro-geological information was further complemented with the lithological map for Switzerland (produced by Swisstopo), which provides a general overview of dominant rock type classes (loose, sedimentary and crystalline rock). The maps are available via opendata.swiss (hydrogeological map, lithological map) or can also be accessed via the Hydrological Service of the FOEN (<https://www.bafu.admin.ch/bafu/de/home/themen/wasser/zustand/karten/geodaten.html>). The number of springs and swallow holes in karstic regions provides additional information related to aquifers and the contribution of subsurface water storage. The layer provides main discharge source locations in karstic regions and is available via opendata.swiss



(produced by FOEN). Standard topographical characteristics such as slope and aspect were derived from the high-resolution digital elevation model (swissALTI3D) publicly available via Swisstopo at a resolution of 2 m (Swisstopo, 2022). The swissTLM3D Hydrography provides topological information on the different water bodies of Switzerland (including flowing and stagnant waters) and originates from the swissTLM3D dataset provided by and accessible via Swisstopo. The biogeographic regions of Switzerland provide six regions differentiated by similarity of flora, fauna, bryophytes and ornithological information as well as homogeneous surface water catchments (BAFU (Hrsg.), 2022). Biogeographic (eco-)regions often correspond well to catchment groups with similar streamflow regime types and are therefore frequently used for catchment regionalization (e.g., Jehn et al., 2020; Guo et al., 2021). The biogeographic regions are available via opendata.swiss.

Finally, general information on the gauging stations and streamflow time series (availability and homogeneity) were provided as accompanying (meta-)data by the FOEN. Time series homogeneity was assessed by a FOEN-internal breakpoint analysis for time series homogenization (for more information see BAFU, 2024). General station information includes catchment area, mean height, glaciation percentage, outlet coordinates and streamflow regime type (among others) (see Figs. 1 and 3). Catchment outlines (polygons provided by the FOEN) and catchment outlets (point shapes) are provided in the coordinate system CH1903/LV03 (EPSG:21781).

4 Data processing

This section describes the methodology used for aggregating spatially gridded data products and catchment descriptors on the catchment level, the methods used to derive additional indicators, standardized drought indices, and presents the definition and declaration of (hydrological) drought events.

4.1 Time series extraction

Based on the spatially gridded hydro-meteorological input products (see Section 3.2), catchment-level time series were extracted using the R-packages *terra* (Hijmans, 2023) and *exactextractr* (Baston, 2023). First, the hourly ERA5-Land data was aggregated to daily resolution following the standards used by the MeteoSwiss spatial climate analyses (e.g., RhiresD and TabsD). For this, instantaneous and accumulation/flux variables are distinguished. For instantaneous variables, we provide daily average values. For accumulation and flux, we provide variables daily sums. Flux variables (mainly precipitation and evapotranspiration) were further aggregated consistently with RhiresD precipitation sums, i.e., from 06 UTC (day) to 06 UTC (day + 1) (see MeteoSwiss, 2021a). Instantaneous variables and ERA5-Land temperature were averaged from 00 UTC to 00 UTC, which is consistent with the other MeteoSwiss products (e.g., TabsD; MeteoSwiss, 2021b). Daily catchment-average time series were then extracted by using the catchment outlines (polygons) provided by the FOEN. Units were homogenized across time series. The units are listed in Table A1.



The length of the time series depends on the dataset that they were derived from (see Table 1 for details). Streamflow time series are provided for three different catchment-specific time periods: 1) the original time series (entire period), 2) the most recent gap-free time-period time series and 3) the most recent homogeneous time series (in case of significant breakpoints; otherwise equal to the gap-free time series) (see Fig. 4). The breakpoint information is provided by FOEN (for more information see BAFU, 2024). Information on the start of the streamflow monitoring by limnographs is also provided. The streamflow data should only be considered reliable after the initialization of a limnograph. In case of no breakpoints the gap-free period is equal to the homogeneous period. The homogeneous period is usually the shortest (e.g., in case of breakpoints or limnograph initialization; see for example catchment 2349 in Fig. 4). In the case of gaps but no breakpoints, both the homogeneous and the gap-free periods are identical (see, i.e., 2239, 2386 and 2368 in Fig. 4). Indicators and (non-)standardized (drought/deficit) indices derived from the hydro-meteorological time series are available for the longest common period of all contributing variables.

4.2 Derived indicators

4.2.1 Streamflow

Derived indicators related to streamflow consist of the 7-day average streamflow (moving average) M7Q. The M7Q (or M7) is often used in low-flow studies and is also used for the official low-flow statistics in Switzerland by the FOEN (see e.g., BAFU, 2024; Muelchi et al., 2021a; von Matt et al., 2024).

4.2.2 Snow related variables

In addition to variables providing direct information on (modelled) snowmelt, also daily differentiated SWE (Δ SWE) time series are provided for both SPASS and OSHD. Snowfall (Δ SWE > 0) and snowmelt (Δ SWE < 0) time series are provided separately. Note that the SPASS SWE is reset at the end of every snow year (every September 1st) to avoid unrealistically high snow water equivalent accumulation (“snow towers”) (Michel et al., 2023). This can result in large snowmelt amounts (Δ SWE < 0) around September 1st. Δ SWE values on September 1st were therefore replaced by a linear interpolation between the day before and the day after. Snow-corrected precipitation series ($P + \Delta$ SWE) were calculated by combining time series of total precipitation (RhiresD and ERA5-Land) and Δ SWE time series (SPASS, OSHD) as well as time series with modelled snowmelt information (SPASS, OSHD and ERA5-Land). Negative snow-corrected precipitation amounts (e.g., RhiresD $< \Delta$ SWE) were set to zero.

4.2.3 Water balance

(Potential) Water balance indicators (P–E and P–PET) were derived by combining the total and snow-corrected precipitation time series with the ERA5-Land evaporation and potential evaporation time series.



240 4.3 Cumulative water deficits

Cumulative (potential) water deficits (CWD and PCWD) are non-standardized indicators tracking evaporation-driven deficits in the (potential) water balance. CWD and PCWD were derived from the daily water balance indicator time series (see Section 4.2.3) using the *cwd* R-package (Stocker et al., 2023; Stocker, 2021). A deficit starts when the water balance is negative (i.e., $P - E < 0$) and is accumulated as long as the deficit remains uncompensated (deficit > 0). Note that no surplus information is tracked. Once the deficit is compensated, the values remain at zero (CWD = 0). In some cases, PCWDs (especially for P–PET based only on ERA5-Land variables) are not compensated each year and can persist over multiple years. Both CWDs and PCWDs are hence also provided on a yearly calculation basis (annual reset on December 31st). Non-standardized indices preserve units (here millimetres) and are physically interpretable in terms of absolute deficit amounts. Cumulative water deficits do not rely on a predetermined calculation time window, which allows the user to track both deficits accumulated over short periods (below one month) and deficits accumulated over very long periods.

4.4 Standardized (drought) indices

Standardized (drought) indices depict the anomaly of a deficit over a fixed retrospective period (e.g., 1 month). The hydrometeorological indicator time series is first aggregated over the given period and then transformed to a standard normal distribution by fitting a suitable candidate distribution (Tijdeman et al., 2020; Stagge et al., 2015). Standardized indices therefore provide information on both anomalously dry and wet conditions, which are often defined by thresholds corresponding to standard deviations (STD). As such, values below -1 STD indicate drier than normal conditions (moderate droughts), while values above $+1$ STD indicate wetter than normal conditions (moderate wetness) (McKee et al., 1993; Tschurr et al., 2020). The HYD-RESPONSES dataset provides daily time series for three standardized (drought) indices: the Standardized Precipitation Index (SPI, McKee et al., 1993), the Snowmelt and Rain Index (SMRI, Staudinger et al., 2014), and the Standardized Precipitation Evaporation Index (SPEI, Vicente-Serrano et al., 2010). SPI and SMRI represent precipitation-driven deficits, as they are based on total (SPI; P only) or snow-corrected (SMRI; $P + \Delta SWE$) precipitation time series. The SPEI accounts for deficits driven by evaporation and is derived from the potential water balance (P–PET). Daily time series for all three indices (SPI, SPEI, SMRI) are provided for aggregation periods ranging from 1–24 months (31–730 days).

All indices were calculated using the *SCI*-package (Stagge et al., 2015; Gudmundsson and Stagge, 2016) with custom modifications accounting for the daily time series resolution. All candidate distributions provided within the *SCI*-package (*gamma*, *genlog*, *gumbel*, *lnorm*, *norm*, *gev*, *pe3*, *weibull*) were tested for suitability. The distributions were fitted for each day of the year (DOY) based on the reference period 1991–2020. The suitability of candidate distributions was assessed based on three indicators: the Shapiro-Wilks normality tests (*p*-values; Shapiro and Wilk, 1965), the number of flags returned by the fitting function (usually indicating convergence issues), and the number of missing and/or implausible values. Implausible values are defined as values above or below $+3$ (-3) STD following Stagge et al. (2015). As in Staudinger et al. (2014), one best-fitting distribution is chosen for all catchments and to allow for catchment comparability. The distribution was selected among the distributions satisfying the following conditions: 1) the transformed values are not significantly different from a normal dis-



tribution for the majority of catchments (p -values > 0.05 for at least 75 % of the catchments), 2) fewer than 5 DOYs flagged and 3) fewer than 50 implausible and/or missing values. The distribution selection procedure is illustrated for the SPEI in Fig. 5. The results of the Shapiro-Wilks tests (p -values) and information on missing/implausible values and flags are also provided in the HYD-RESPONSES dataset and can be used to identify catchments with non-satisfying properties within the overall best-fitting distribution (see Fig. 5).

The *Gamma* distribution was chosen for the SPI for all variables (RhiresD, ERA5-Land), which is consistent with other studies and WMO recommendations (WMO and GWP, 2016; Stagge et al., 2015; Tschurr et al., 2020; von Matt et al., 2024). The SMRI was fitted by the *genlog* (*lnorm*) distribution for the snow-corrected precipitation series based on SPASS (ERA5-Land and OSHD). For the SPEI, the *genlog* distribution was found to perform best across time scales (see Fig. 5). Following Stagge et al. (2015), values of all standardized (drought) indices time series were restricted to the interval $[-3, 3]$ STD.

4.5 Climatology & Anomalies

Climatologies and anomalies are provided for all time series including the standard time series of extracted variables (see sections 3.1 and 3.2, derived indicators (Section 4.2), standardized (drought) indices (Section 4.4) and cumulative water deficits (Section 4.3 and 4.6). Both climatologies and anomalies are based on the reference period 1991–2020. The climatology is provided for two variants: i) using moving windows and ii) for fixed periods. The variants are available at the following time scales: daily (only i), monthly (both), seasonal (both), and annual (only ii). The moving window climatology was calculated by using a moving window of 31 days ($day - 15$, $day = 0$, $day + 15$) for the monthly, a 3-month window (91 days) for the seasonal and a 6-month (183 days) window for the extended season time scale. The moving window climatology is calculated for DOYs 1–366 with NA-values set for February 29th in the case of non-leap years. The regular climatology is available for monthly, seasonal (DJF, MAM, JJA, SON), extended season (Mai–October, November–March) and annual time scales. Using the moving window climatology, standardized anomalies have been derived by calculating z-scores $((value - \mu)/\sigma)$. The following climatological statistics are provided: minimum, maximum, mean, median, standard deviation, 5th, 25th, 75th and 95th percentiles. For the 7-day average streamflow series (M7Q) we also provide the 2nd, 10th and 15th percentiles.

4.6 Cumulative streamflow deficits

Time series of cumulative streamflow deficits (CQD) were calculated based on negative streamflow anomalies (drought phases) by using the same procedure as for cumulative water deficits (see Section 4.3). CQD time series are provided for both fixed and variable threshold definitions. For the fixed threshold definition, daily M7Q anomalies were derived for the yearly Q347-threshold events (\approx the yearly 5th percentile, see Section 5.2). For the variable threshold definition, daily M7Q anomalies were calculated for the following monthly (31 days) and seasonal (91 days) percentiles: 2nd, 5th, 10th, 15th, 25th, 50th (median) and mean. Cumulative deficits are physically interpretable and in the case of cumulative water deficits [mm] and streamflow deficits [m³/s] also physically comparable in terms of total runoff depth [mm].



4.7 Identification of drought events

We define drought events as coherent phases of non-zero deficits for cumulative deficits (CWD, PCWD and CQD) and as negative M7Q-based streamflow anomalies for streamflow droughts. Streamflow drought phases were extracted for the same percentiles and time scales as used for CQDs (see section 4.6), namely for monthly (31 days) and seasonal (91 days) percentiles: 2nd, 5th, 10th, 15th, 25th, 50th (median) and the mean. For each event definition, the event time series consists of consecutively numbered event phases and information on the event duration since the start. A minor pooling for hydrological drought events is introduced by using 7-day average streamflow (M7Q) (Tallaksen and Van Lanen, 2004; Hisdal and Tallaksen, 2000; Tallaksen et al., 1997; Sarailidis et al., 2019).

5 Catchment descriptors

Catchment descriptors were extracted from spatial datasets containing information on hydro-terrestrial characteristics (e.g., soil suitability maps), catchment (station) metadata (see Section 3.3) and the extracted hydro-meteorological time series (e.g., climatology; see Section 4.5). All catchment descriptors provide only static (time-invariant) catchment information. Catchment descriptors are provided as single-value catchment-level information.

5.1 Extraction of catchment descriptors

Spatially non-overlapping polygon datasets (e.g., soil suitability maps) typically provide categorized values for variable-specific classes (e.g., soil depth classes are *shallow*, *medium*, *deep*, *very deep*). To extract catchment-level information, polygon-based information was first rasterized to a spatial grid identical to the MeteoSwiss spatial climate analyses grid products (in both extent and resolution). The rasterization was done by using the *rasterize* function of the *terra* R-package (Hijmans, 2023). Each grid cell only contains the value of the category with the largest overlap. Slope and aspect values were derived from the swissALTI3D digital elevation model (DEM, see section 10 for a download link) by using the standard *terra* R-package function *terrain* (Hijmans, 2023). A custom categorization was then applied to the resulting grid values (e.g., for slope 0–30, 30–60, etc.). The percentage overlap with the catchment area was then assessed for all variable-specific classes by using the *exact_extract* function (as for time series) and adjusting the aggregation function to fractions ("frac"; see Baston, 2023). Catchment area overlap fractions are provided for all categories. Descriptors with multiple classes can also be reduced to a single dominant category represented by the largest percentage overlap ("proportion"). An example is shown for the biogeographic regions in Fig. 7. However, the class with the largest overlap does not necessarily correspond to the most representative, as multiple categories can share similar proportions of the catchment area.

5.2 Derivation of other catchment descriptors

Additional catchment descriptors were derived from the remaining descriptive input products (catchment metadata, karstic sources, catchment outlines and hydrography) and the calculated hydro-climatology (see Section 4.5).



Two descriptive variables related to catchment shape and drainage were derived in R by using the catchment outlines, namely
 335 the *basin shape index* (BSI) and *drainage density*. The HYD-RESPONSES dataset provides two BSI variants. The first variant
 is derived based on a ratio between area and length (A/L^2) and the second variant is based on a ratio between the catchment area
 and the area of the circle with the smallest radius encircling the entire catchment (A_{catch}/A_{circle}). For more information see
 Das et al. (2022). The drainage density denotes the ratio between the catchment area and the total length of streamflow channels
 (both natural and stormwater drainage infrastructure; Dingman, 1978; USGS, 2023). The drainage density was calculated by
 340 using the swissTLM3D hydrography dataset (see section 10 for a download link). Both indices (BSI and drainage density) are
 frequently used in flood-related studies but may also provide valuable information during low-flow periods as high-intensity
 precipitation events are a relevant factor for (streamflow) drought recovery (Eekhout et al., 2018; Floriancic et al., 2022; Lee
 and Ajami, 2023; Matanó et al., 2024; Qiu et al., 2021; Tarasova et al., 2024; Vicente-Serrano et al., 2022; Wu et al., 2022;
 Xu et al., 2023). Further, also the overlap percentage with the Swiss territory (swissBOUNDARIES3D, see section 10 for a
 345 download link) is provided for each catchment and can be used to exclude catchments with significant portions outside of
 Switzerland which goes along with a limited coverage in both hydro-meteorological and catchment descriptor input datasets
 (see Sections 3.2 and 3.3). Information on karstic sources is provided as the number of sources per catchment and km^2 .

Several indices related to streamflow characteristics (low flow, responsiveness, baseflow and flow stability) are provided in
 the HYD-RESPONSES dataset. The Q347 (Aschwanden, 1992; Aschwanden and Kan, 1999) is a low flow index used as the
 350 basis for water abstraction restrictions in Switzerland and corresponds to the 5th streamflow percentile (low flows) derived
 from the flow duration curve (FDC). The Q347 was derived by using the *hydroTSM* R-package (Zambrano-Bigiarini, 2020).
 The baseflow index (BFI; Nathan and McMahon, 1990) is a widely used index linked to multiple catchment characteristics
 such as aquifer type, productivity and soil characteristics. The BFI provides information on the (base-)flow sustained during dry
 periods (e.g., by subsurface storages; Tallaksen and Van Lanen, 2004; Bloomfield et al., 2021; Van Loon and Laaha, 2015). The
 355 BFI was derived using the *baseflow* function of the *lfstat* R-package (Laaha and Koffler, 2022) and is shown in Fig. 7. Stoelzle
 et al. (2020) introduced the delayed-flow index (DFI) which breaks down the BFI into individual hydrograph components. The
 components include fast, intermediate, slow and base responses and potentially reflect various storage processes contributing to
 the overall streamflow response (e.g., snowmelt and groundwater). The DFI was derived by using the *delayedflow* R-package
 (<https://modche.github.io/delayedflow/>; see also Stoelzle et al., 2020). The last two indices related to streamflow behaviour
 360 are the "flashiness" or R-B-index (Baker et al., 2004) which represents the ratio of the sum of day-to-day streamflow changes
 divided by the total streamflow and the flow-stability index which relates the mean annual minimum flows to the mean annual
 flow (MAM/MQ).

The remaining catchment descriptors were derived from the extracted hydro-meteorological time series and/or their respective
 climatology. Information on average precipitation, temperature, evaporation, snow water equivalent, streamflow, the fraction of
 365 precipitation falling as snow and the runoff fraction (Q/P) are provided, partly on both monthly and yearly time scales. Finally,
 monthly Pardé coefficients (PCs) are provided which indicate the contribution of monthly mean streamflow to the annual mean
 streamflow.



6 Three example use cases

The different data types can be combined to comprehensively analyse hydrological streamflow droughts in response to various hydro-meteorological indicators. This section presents three use cases: catchment regionalization, in-depth event analysis, and composite analysis. A comprehensive R-tutorial on how to read and combine the different data products is provided with the dataset but can also be accessed via Github (<https://github.com/codicolus/HYD-RESPONSES>).

6.1 Catchment grouping

For some applications, catchments need to be grouped by similarity, as measured by a set of hydro-meteorological, terrestrial and/or anthropogenic catchment descriptors (e.g., Tarasova et al., 2024). As an example application, we show the distribution of catchment coverage fractions across biogeographic regions for the soil characteristics *soil depth*, *skeletal content*, *water logging*, *permeability*, and *water storage capacity* (Figure 8).

The percentage coverage distributions reveal notable differences in soil characteristics and their subcategories. Catchments in the Swiss Plateau region are characterized by larger coverages of deep to very deep soils with a mostly poor to medium skeletal content, normal soil permeability and good water storage capacities (see Fig. 8). Alpine catchments, on the other hand, are characterized by shallower soils (especially the Southern Alps) and a higher skeletal content. Soils in the Alps further have almost no water logging and a low water storage capacity. Soils with a (weakly) inhibited permeability or with a very good water storage capacity are infrequent across all biogeographic regions. An other example for catchment grouping is the streamflow regime type classification for Switzerland (see e.g., Aschwanden and Weingartner, 1985; Weingartner and Schwanbeck, 2020). Figure A1 in Appendix A shows the incidence of streamflow regime types across biogeographic regions.

6.2 Detailed Event analysis

The combination of hydro-meteorological indicators, standardized (drought) indices (SPI, SPEI, SMRI), cumulative (potential) water (balance) and streamflow deficits (CWD, PCWD, CQD) and accompanying climatological anomalies allow for a detailed analysis of specific (streamflow) drought events. Drought-generating processes vary across catchments depending on hydro-climatological and terrestrial catchment characteristics, the season as well as on anthropogenic disturbances (e.g., Brunner et al., 2022; Van Loon and Van Lanen, 2012; Van Loon, 2015; Apurv et al., 2017). Except for glacier melt and groundwater, the HYD-RESPONSES dataset provides time series for all relevant hydro-meteorological indicators required to analyse (streamflow) drought generation, drought propagation as well as drought type classification.

Figure 9 illustrates time series for the year 2022 of a subset of relevant hydro-meteorological variables for catchment 2034 - Broye, Payerne, Caserne d'aviation. This catchment is located in the western Swiss Plateau region (highlighted in Fig. 2). The year 2022 was an exceptional year with unprecedented combined heat and drought conditions over Europe (Tripathy and Mishra, 2023). The Broye catchment experienced low-flow conditions beyond a 100-year return period (BAFU (Hrsg.), 2023). In the Broye catchment, the lowest 7-day average streamflow values were observed between July and August (see Fig. 9i) Several streamflow drought events were identified for both yearly fixed (purple shading) and variable (green shading)



400 threshold definitions. The longest events occur during the annual low-flow season for both definitions.

The year 2022 was also one of the warmest years on record with three heatwaves occurring in mid-June, mid-July and in the beginning of August (Imfeld et al., 2022). During the longest streamflow drought event in July 2022 (M7Q row in Figure 9i), evaporation anomalies begin to decline and become negative towards the end of the event (ET row in Fig. 9c). Concurrent strong negative soil moisture anomalies at shallow and deeper levels (see Fig. 9d) suggest that the successively decreasing
 405 evaporation anomalies may be related to increasingly depleted soil moisture storages resulting in limited water availability for evaporation. Interactions between (subsurface) storage processes are however complex and also include groundwater–soil moisture interactions (e.g., Orth and Destouni, 2018).

The HYD-RESPONSES dataset further provides information on cumulative (atmospheric) water deficits represented by standardized and non-standardized (drought) indices. For the Broye catchment, the 2022 streamflow drought events identified
 410 with the variable threshold (green shading) correlate well with shorter aggregation scales (1- to 3-monthly) SPI and SMRI indices in spring and summer. The correspondence between short-term precipitation deficits and streamflow droughts is, however, not consistent throughout the year. During the variable threshold streamflow droughts in mid-March to April, both SMRI-1 and SMRI-3 reach more negative values than their SPI equivalents, which suggests a contribution of lacking snowmelt to the streamflow drought generation (see Fig. 9g,h).

415 Cumulative deficits in actual (CWD, Fig. 9k) and potential (PCWD, Fig. 9l) water balance as well as streamflow (CQD, Fig. 9j) provide complementary information to the SPI, SMRI and SPEI in the form of non-standardized and hence physically interpretable deficit amounts. Cumulative streamflow deficits (CQD) show only two phases without deficit compensation for both drought definitions (Fig. 9j). A shorter CQD phase coincides with the drought events in spring (variable threshold) and the shorter drought event in June (fixed threshold), while a longer phase coincides with the remaining shorter and longer streamflow
 420 drought phases in July and August before CQD is compensated by September 2022. For both CQD phases, the CQD is larger for streamflow droughts based on a variable threshold definition. Above average precipitation (+130 %; BAFU (Hrsg.), 2023) was reported in September 2022 and corresponds well with the compensation of CQD and is also reflected in the positive monthly (31d) precipitation anomalies (P anomaly, Fig. 9b). Similar to the longest streamflow drought phases, also the largest deficits in (actual) water balance (CWD) occurred between May–August 2022. Larger CWDs during the warm season are consistent with
 425 the seasonal climatology of both temperature and evaporation with the highest values during summer (not shown). Major CWD phases match streamflow drought phases remarkably well, especially for the variable threshold definition with one exception in April. The two longer streamflow drought phases in May–June further show the benefits of considering anomalies in the CWDs. While absolute CWDs were not compensated in between the streamflow droughts, the CWD anomalies indicate that the deficits returned to seasonal norm values (see Fig. 9m). Cumulative deficits in potential water balance (PCWDs, Fig. 9l) are
 430 more similar to cumulative streamflow deficits (CQD) for the variable-threshold definition. This reflects the different nature of CWDs and PCWDs. The actual water balance is more strongly tied to the actual water availability and hence the individual streamflow phases. The potential water balance, on the other hand, represents the deficit that would have been accumulated under unlimited water availability. Similar to PCWD, CQDs reflect the integrated streamflow deficit over time while an actual deficit in terms of low streamflow levels does not necessarily have to exist (anymore).



435 6.3 Composite analysis (catchment response patterns)

Composite analysis is a frequently used approach to understand the driving processes of a phenomenon such as droughts (see e.g., Bevacqua et al., 2021; Floriancic et al., 2020; Mahto and Mishra, 2024). By considering the median values of drought indicators across all streamflow drought events in a catchment, typical response patterns may become more evident and may allow for more generalized inferences on typical streamflow drought response patterns e.g., to precipitation deficits accumulated over various aggregation time-scales. Here, we present a composite analysis of median SPI values associated with streamflow droughts defined by the monthly 15th-percentiles of the streamflow.

Note that streamflow drought characteristics and drought propagation processes may differ among catchments depending on hydro-meteorological climatologies, geological and terrestrial characteristics (e.g., aquifer, rock type, (soil) water storage capacity), seasonality of and differences in contributing streamflow (drought) generating processes and human disturbances (e.g., Van Loon and Laaha, 2015; Floriancic et al., 2022; Jehn et al., 2020; Apurv and Cai, 2020; Savelli et al., 2022; Haile et al., 2020; Brunner et al., 2022, 2021, 2023; Tjiedeman et al., 2022; de Jager et al., 2022). We therefore separate the streamflow droughts and catchments by seasons winter (DJF, December–February), spring (MAM, March–May), summer (JJA, June–August) and autumn (SON, September–November) and by streamflow regime types. Six streamflow regime types are selected to capture a variety in dominant streamflow (drought) generating processes. These include glacial (*a-glaciaire*, *nivo-glaciaire*), nival (*nival alpin*, *nival méridional*) and pluvial (*pluvial jurassien*, *pluvial supérieur*) processes. The importance of precipitation deficits across scales is assessed using SPIs (SPI-1 to SPI-24). Streamflow drought events are only considered for the longest common homogeneous period across catchments (1991–2022). The selection is further restricted to catchments with at least 10 streamflow drought events in each season (over the entire time series length) with a minimum duration of at least 10 days to enhance robustness and exclude minor droughts.

Median SPI values are mostly negative across all aggregation time-scales indicating that precipitation conditions co-occurring with streamflow droughts tend to be drier than normal. Several streamflow regimetype-specific response patterns are evident and change across seasons along with contributing streamflow (drought) generating processes.

Glacier melt is the dominant factor for the *a-glaciaire* regime type. Streamflow levels are typically lowest in winter (January–March) as a result of precipitation falling as snow (intermediate storage) and highest in summer due to large contributions of glacier melt (Aschwanden and Weingartner, 1985; Weingartner and Schwanbeck, 2020; Muelchi et al., 2021b). Streamflow droughts of strongly glaciated catchments are not associated with moderate drought conditions at any SPI scale. In glacial and nival catchments a shift towards short-term precipitation deficits (SPI-1 to SPI-6) being associated with droughts is present across seasons and drought-generating processes. The transition towards shorter deficit scales emerges in summer for nival regime types and in autumn for glacial regime types. In pluvial and transitional regime types short-term precipitation deficits (mostly 1- to 3 months) are relevant throughout the year. Seasonal shifts are also observed for pluvial and transitional regime types with mid- and long-term precipitation deficits becoming more relevant in summer and autumn.

In addition to 3-monthly precipitation deficits, also mid- and long-term deficits become relevant in summer and autumn for (nivo-pluvial) catchments in the Jura region and catchments of the regime type *pluvial inférieur*. Compound moderate droughts



are mainly observed for sub-yearly (1- to 9-monthly) scales with most extreme conditions on a 6-monthly scale in the Jura region (especially for nivo-pluvial catchments) and on a (6- to) 9-monthly scale for catchments of the regime type *pluvial inférieure*. In southern Switzerland, precipitation deficits tend to be relevant on longer scales compared to similar regime types north of the Alps. In contrast to nival catchments north of the Alps (*nival alpin*), droughts in the nival catchments south of the Alps (*nival méridional*) are associated with substantial precipitation deficits at longer aggregation times (9–24 months). The deficits occur in winter and in summer, but conditions are more extreme in summer ($SPI \approx -1.5$) on scales longer than 15 months. Further, also 3-monthly precipitation deficits appear to be relevant for streamflow (drought) generation in summer (moderate drought conditions). In spring and autumn, mid- to short-term accumulation scales are more relevant. Interpretations of the differences between the south and north sides of the Alps should however be considered with caution due to the small catchment sample sizes and the spatial proximity of the two *nival méridional* catchments. The observed response patterns may therefore not be representative of nival catchments south of the Alps in general.

7 Discussion

The HYD-RESPONSES dataset can, for example, be used to study drought dynamics and drought propagation, for streamflow forecasting using Long Short-Term Models Kratzert et al. (LSTMs; 2018); Lees et al. (LSTMs; 2022); Kratzert et al. (LSTMs; 2023), Random Forests Floriancic et al. (RFs; 2022), or to infer drought drivers using clustering and principal component analysis (e.g., Jehn et al., 2020). The information on breakpoints allows to study pre- and post-influence catchment behaviour e.g., by using the paired catchment or upstream-downstream approach (see e.g., Rangelcroft et al., 2019; Van Loon et al., 2019). The availability of variables originating from multiple data sources (direct observations, reanalysis data, model data) allows for comparative analyses. The following variables are available from multiple sources: temperature (MeteoSwiss, ERA5-Land), precipitation (MeteoSwiss, ERA5-Land), and snow (MeteoSwiss, WSL, ERA5-Land).

There are several known limitations related to the datasets used to compile the HYD-RESPONSES data. ERA5-Land is a state-of-the-art reanalysis product provided at a higher spatial resolution than the standard ERA5 reanalysis (Hersbach et al., 2020; Muñoz-Sabater et al., 2021). The higher spatial resolution results in a better depiction of soil moisture, lakes, river discharge estimations, and the orographic enhancement of precipitation (Muñoz-Sabater et al., 2021). However, the grid resolution of 9 km still has limitations over complex high-altitude terrain. The extracted time series related to snow depth (SWE) should be used with caution, as snow depth in ERA5-Land is of mixed quality depending on geographical location and altitude (Dalla Torre et al., 2024). Scherrer et al. (2023) showed, that ERA5-Land overestimates SWE at high elevations with larger biases in the southern compared to the northern Alps. They state that higher-resolution datasets such as SPASS (Marty et al., 2025) and OSHD (Mott, 2023; Mott et al., 2023) should be preferred over ERA5-Land. Further also note that all snow-related datasets have problems in representing small SWE amounts at low altitudes (Scherrer et al., 2023; Michel et al., 2023; Marty et al., 2025).

Another limitation of the ERA5-Land dataset is the parameterization of subgrid-scale processes and the representation of subsurface storages that affect evapotranspiration (e.g., fixed maximum storage volume assumption; see Muñoz-Sabater et al.,



2021). However, gridded observation-based evaporation datasets are yet to be developed for Switzerland.

Caution is required when using the snow-corrected precipitation (water input) time series. The time series corrected by the Δ SWE series consider both snowfall (Δ SWE > 0) and snowmelt (Δ SWE < 0), while the correction based on snowmelt variables only accounts for snowmelt (*smlt* in ERA5-Land and *romc* in OSHD; see Table 1 and Table A1). Snowmelt-corrected precipitation time series only account for snowmelt, they may, therefore, be of limited use during the main snow accumulation season but can still provide valuable information during the snowmelt season.

The time series for standardized (drought) indices are only provided for the transformation based on the best-fitting distribution across all catchments to allow for catchment comparability (see e.g., Staudinger et al., 2014). The best-fitting distribution may however vary across catchments and climates (see e.g., Stagge et al., 2015). The HYD-RESPONSES dataset provides information on fits, missing values and flags which can be used to exclude catchments with unsatisfying fitting and transformation properties from analyses.

The HYD-RESPONSES time series are provided for product-specific periods and the spatial coverage is restricted to Swiss territory for most of the higher resolution MeteoSwiss and SLF products (TabsD, TminD, TmaxD, SPASS, SrelD, OSHD) as well as many catchment descriptor input datasets. Full coverage over the entire hydrological Switzerland is only available for ERA5-Land (all variables) and the MeteoSwiss RhiresD product (after 1992; see MeteoSwiss, 2021a). Catchments with significant areas outside of the Swiss National borders may therefore be considered with caution or excluded from the analysis.

8 Complementary datasets

Complementary datasets provide a wide range of additional catchment descriptors and hydro-meteorological time series. An overview of datasets and variables is provided in Table 3. The FOEN provides additional geodata related to both surface and groundwater via the Hydrological Service (<https://www.bafu.admin.ch/bafu/de/home/themen/wasser/zustand/karten/geodaten.html>). The datasets include additional catchment descriptors with information on population density, catchment areas covered by forest and agriculture (among others) as well as information on water quality aspects and sewage. The FOEN further operates both a groundwater monitoring network (NAQUA) providing continuous groundwater measurements for selected point locations (BAFU, 2019) and a water quality measurement network (NAWA) providing information on concentration and loads of important dissolved compounds (e.g., pH, electric conductivity, nutrient contents; BAFU, 2023).

The “Catchment Attributes and Meteorology for Large-sample catchment Studies” (CAMELS) datasets aim at providing a consistent set of hydro-meteorological time series and catchment descriptors over a large sample of hydrological catchments on country level (Clerc-Schwarzenbach et al., 2024). The catchments in the Swiss version of the CAMELS data (CAMELS-CH; Höge et al., 2023a) are largely congruent with our dataset. The only exception is station 2646, which is only contained in the HYD-RESPONSES dataset. Note that the HYD-RESPONSES dataset provides only a sample subset of 184 catchments. The CAMELS-CH dataset provides valuable complementary catchment-level information on glacier changes (based on GLAMOS, for details see Höge et al., 2023a), land use, hydro-geological and hydro-terrestrial information (e.g., the contributions of vari-



Table 3. Datasets compatible and complementary to the HYD-RESPONSES dataset.

Dataset	Short description	Provider
Accompanying catchment information	Includes catchment proportions of forests, agricultural (crop) land, population, built-up area and more	FOEN
Groundwater measurement network (NAQUA)	Groundwater measurements	FOEN
Water quality measurement network (NAWA)	Information on water quality parameters	FOEN
CAMELS-CH	Swiss version of the Catchment Attributes and Meteorology for Large sample catchment Studies (CAMELS) dataset	Zenodo
MeteoSwiss CombiPrecip (CPC)	High-resolution precipitation fields at ground based on a combination of radar and measurement data	MeteoSwiss
HydCheck	Detailed evaluation of influences and disturbances of the streamflow at NAWA measurement stations	FOEN

ous grain size categories and bulk-density) as well as anthropogenic disturbances (e.g., hydropower and reservoir capacities). CAMELS-CH further provides modelled time series based on the hydrological model PREVAH (see e.g., Höge et al., 2023a; Viviroli et al., 2009). The CAMELS-CH dataset is freely available from Zenodo (<https://zenodo.org/records/10354485>; Höge et al., 2023b).

The CombiPrecip dataset (MeteoSwiss) provides high-resolution (10 minutes, 1×1 km) precipitation fields derived from a combination of radar and station measurement data (Sideris et al., 2014). The CombiPrecip dataset could be a valuable addition for studying drought recovery where extreme precipitation is often considered an important factor (Wu et al., 2022).

The HydCheck project (Streeb et al., 2024) evaluated the influence of (anthropogenic) disturbance factors on streamflow at stations of the National Surface Water Quality (NAWA) Programme (BAFU, 2023). The evaluated NAWA stations are largely (87.5% of the stations) congruent with the HYD-RESPONSES dataset. The HydCheck dataset provides catchment-level information on the magnitudes for all evaluated disturbance categories including water storage and regulation, hydropower, sewage water, constructions, agriculture as well as drinking and groundwater. The overall impact on several hydrological properties including low-, mid- and high-flow regimes as well as short-term effects and hydraulics is provided as categorical information (from "not disturbed" to "strongly disturbed"). For more information see Streeb et al. (2024).

As part of the planned Swiss National drought early warning system (DEWS), both a high-resolution remote-sensing based evaporation product (V. Humphrey, pers. comm.) and an automatic soil moisture measurement network are under development at MeteoSwiss, ETH Zurich and WSL and may become a valuable addition in a future.



9 Conclusions

The HYD-RESPONSES dataset contains data for 184 Swiss catchments that cover a variety of streamflow regimes, mean altitudes, catchment areas, and anthropogenic influences/disturbances. The catchments cover all biogeographic regions of Switzerland. The HYD-RESPONSES dataset provides daily streamflow data and daily hydro-meteorological time series extracted from gridded data products of MeteoSwiss (TabsD, RhiresD, TmaxD, TminD, SrelD), Meteoswiss and SLF (SPASS), SLF (OSHD) and ECMWF (ERA5-Land). The variables include temperature, precipitation, evaporation, sunshine duration, solar radiation, snowmelt, snow water equivalent, soil moisture, surface runoff, runoff, and streamflow. HYD-RESPONSES further provides derived variables related to streamflow (e.g., M7Q), water balance (e.g., P–E) and snowfall. Additionally, three standardized drought indices (SPI, SPEI, SMRI) for accumulation periods from 1 to 24 months and information on the (non-standardized) cumulative water deficit (CWD), the potential cumulative water deficit (PCWD) and cumulative streamflow deficit (CQD) are provided.

The data set also provides information on (streamflow) drought events (occurrence and duration). For each catchment, the drought events have been identified based on fixed and on seasonally varying percentile thresholds. The combination of data sources, the information on hydro-meteorological variables (mainly temperature, precipitation and snow), the derived indices (water balance, cumulative water deficits, standardized drought indices, climatology and anomalies) allow for a multi-purpose use and various analytical approaches such as time series analysis (e.g., Kratzert et al., 2018; Lees et al., 2022), drought propagation and catchment sensitivity analysis (e.g., based on principal component analysis and clustering; Jehn et al., 2020) and changes in rainfall-runoff relationships during hydrological droughts (e.g., Wu et al., 2021). The HYD-RESPONSES data set can easily be combined with complementary datasets such as CAMELS-CH (Höge et al., 2023a) and HydCheck (Streeb et al., 2024). The catchment time series vary in length (subject to station initialization), the hydrological time series are provided for the entire measurement period along with information on data homogeneity (see BAFU (2024) for more details).

Limitations exist for catchments extending beyond the Swiss borders. The catchment descriptors were extracted from datasets only covering Swiss national territory. The MeteoSwiss-based datasets cover only Switzerland except for RhiresD, which covers the entire hydrological Switzerland from 1992 onward. In summary, the data set provides a state-of-the-art data basis to study droughts in Switzerland.

Code and data availability. The HYD-RESPONSES dataset is freely available (CC BY 4.0) from Zenodo (<https://doi.org/10.5281/zenodo.14713274>; von Matt et al., 2025). Regular updates are not planned. An R tutorial on how to use and combine the different data products is provided with the dataset but can also be accessed on GitHub (<https://github.com/codicolus/HYD-RESPONSES>).

As of now, MeteoSwiss gridded spatial analyses products (MeteoSwiss, 2021a, b, c) are not available for free but will be available for free in the course of 2025 (MeteoSwiss, 2025). The preliminary snow climatology for Switzerland (SPASS; see Michel et al., 2023; Marty et al., 2025) was provided directly by MeteoSwiss and is not yet available for public use. The SLF snow climatology (OSHD; Mott, 2023; Mott et al., 2023) was published under the WSL Data Policy and can be downloaded via



585 Envidat (<https://www.envidat.ch/#/metadata/climatological-snow-data-1998-2022-oshd>). The hourly ERA5-Land dataset (Muñoz-Sabater et al., 2021) is accessible via the Copernicus Climate Data Store (CDS) (see <https://cds.climate.copernicus.eu/datasets/reanalysis-era5-land?tab=download>). Daily streamflow time series can be requested via the Hydrological Service of the FOEN via <https://www.bafu.admin.ch/bafu/de/home/themen/wasser/zustand/daten/messwerte-zum-thema-wasser-beziehen.html>. The soil suitability maps (FOAG), the hydrogeological map (FOEN) and the lithological map (Swisstopo) are available from <https://opendata.swiss> or
 590 directly via Swisstopo (<https://www.swisstopo.admin.ch/de/geokarten-500-vektor>). Directly available from Swisstopo are also the datasets swissALTI3D (<https://www.swisstopo.admin.ch/de/hoeihenmodell-swissalti3d#swissALTI3D---Download>), swissTLM3D Hydrography (<https://www.swisstopo.admin.ch/de/landschaftsmodell-swisstlm3d#swissTLM3D---Download>) and swissBOUNDARIES3D (<https://www.swisstopo.admin.ch/de/landschaftsmodell-swissboundaries3d>). Further available via <https://opendata.swiss> are the Biogeographic regions (<https://opendata.swiss/de/dataset/biogeographische-regionen-der-schweiz-ch>; see also BAFU (Hrsg.), 2022) and information on
 595 karstic springs and swallow holes (also produced by the FOEN; <https://opendata.swiss/de/dataset/quellen-und-schwinden-in-karstgebieten>). Data used for the overview map of the study region (Fig. 1) is available for free from Swisstopo and FOEN. Datasets used include: the digital height model DHM25 (<https://www.swisstopo.admin.ch/de/hoeihenmodell-dhm25>) and the general hydrological background map (downloadable via <https://opendata.swiss>; see <https://opendata.swiss/en/dataset/generalisierte-hintergrundkarte-zur-darstellung-hydrologischer-daten>).

600 The software used to compile the datasets are all open-source and contain the following R-packages available via CRAN: *tidyverse* (<https://cran.r-project.org/web/packages/tidyverse/index.html>; Wickham et al., 2019), *exactextractr* (<https://cran.r-project.org/web/packages/exactextractr/index.html>; Baston, 2023), *sf* (<https://cran.r-project.org/web/packages/sf/index.html>; Pebesma, 2018), *lfstat* (<https://cran.r-project.org/web/packages/lfstat/index.html>; Laaha and Koffler, 2022), *SCI* (<https://cran.r-project.org/web/packages/SCI/index.html>; Gudmundsson and Stagge, 2016; Stagge et al., 2015) and *stars* (<https://cran.r-project.org/web/packages/stars/index.html>; Pebesma and Bivand, 2023).
 605 Available via Github are the R-packages *cwd* (Stocker (2021); available via: <https://github.com/stineb/cwd>), and *delayedflow* (Stoelzle et al. (2020); available via: <https://modche.github.io/delayedflow/>).

Author contributions. CNvM conceptualized the project proposal, acquired funding from the FOEN, performed the formal analysis and wrote the article. OM and BS provided guidance on the methodological aspects. CNvM, OM and BS assisted with writing the paper and
 610 revisions.

Competing interests. The contact author has declared that none of the authors has any competing interests.

Acknowledgements. The HYD-RESPONSES project was funded by the Federal Office for the Environment (FOEN). The preliminary SPASS dataset was kindly provided by Regula Muelchi (MeteoSwiss). We thank Caroline Kan (FOEN) for her help with the catchment selection.



Table A1. Glossary of extracted time series variables, their description and units.

Dataset	Variables	Variables (fullname)	Units	Producer
Spatial Climate Analyses	TabsD	Daily 2 m mean temperature	°C	MeteoSwiss
	RhiresD	Daily precipitation sums	mm	
	TminD	Daily 2 m minimum temperature	°C	
	TmaxD	Daily 2 m maximum temperature	°C	
	SrelD	Daily sunshine duration	%	
Snow Climatology for Switzerland (SPASS)	SWECLQMD	Daily snow water equivalent	mm	MeteoSwiss & SLF
Climatological snow data since 1998 (OSHD)	swee	Daily snow water equivalent	mm	SLF
	romc	Daily snowmelt-contribution to runoff	mm	
ERA5-Land	tp	Total precipitation	mm	ECMWF
	t2m	Average 2 m temperature	°C	
	e	Total evaporation	mm	
	pev	Total potential evaporation	mm	
	smlt	Snowmelt	mm	
	sd	Snow water equivalent	mm	
	ssr	Total solar radiation	MJ/m ²	
	ro	Runoff	mm	
	sro	Surface runoff	mm	
	swv11	Soil water volume level 1 (0–7cm)	mm	
	swv12	Soil water volume level 2 (7–28cm)	mm	
	swv13	Soil water volume level 3 (28–100cm)	mm	
	swv14	Soil water volume level 4 (100–289cm)	mm	
Streamflow time series	Q	Daily mean streamflow	m ³ /s	FOEN

Appendix A



Table A2. Characteristics of all 184 catchments in the HYD-RESPONSES dataset (Part 1/5).

Catchment	Water name	Place	Lon / Lat EPSG:21781	Glaciation %	Area km ²	Avg. Height m asl	Regime Type	Yearly Avg. T °C	Yearly P mm	Yearly E mm	Yearly Q mm
0070	Emme	Emmenmatt	623610 / 200420	0.0	443.00	1065	nivo-pluvial préalpin	6.94	1539.26	300.29	856.45
0078	Poschiavino	Le Prese	803490 / 130520	4.0	168.00	2162	nival méridional	1.58	1324.78	175.84	1078.26
0155	Emme	Wiler, Limpachmündung	608220 / 223240	0.0	937.00	858	mixed regime (>500km ²)	7.80	1356.58	313.03	623.66
0185	Plessur	Chur	757975 / 191925	0.0	264.00	1868	nival alpin	3.42	1179.00	194.41	915.28
0308	Goldach	Goldach, Bleiche	753190 / 261590	0.0	51.10	827	pluvial supérieur	8.33	1423.14	317.59	889.48
0352	Linth	Linthal, Ausgleichsbecken KLL	718285 / 197310	9.4	147.00	2085	a-glacio-nival	1.83	1874.45	169.98	2422.14
0403	Inn	Cinuos-chel	797700 / 168170	5.2	733.00	2456	mixed regime (>500km ²)	-0.66	1007.10	146.31	1007.68
0488	Simme	Latterbach	610680 / 167840	1.5	563.00	1594	nival de transition	4.79	1506.56	225.96	1108.96
0491	Schächen	Bürglen, Galgenwäldli	692480 / 191800	1.5	108.00	1728	nivo-glaciaire	3.55	1854.00	188.20	1646.44
2009	Rhône	Porte du Scex	557660 / 133280	11.0	5238.00	2127	mixed regime (>500km ²)	1.96	1292.71	148.24	1116.86
2011	Rhône	Sion	593770 / 118630	14.2	3372.00	2291	mixed regime (>500km ²)	1.00	1240.59	127.84	966.98
2016	Aare	Brugg	657000 / 259360	1.5	11681.00	1000	mixed regime (>500km ²)	7.34	1317.32	291.55	833.95
2018	Reuss	Mellingen	662830 / 252580	1.8	3386.00	1259	mixed regime (>500km ²)	5.98	1592.79	239.54	1300.70
2019	Aare	Brienzwiler	649930 / 177380	15.5	555.00	2135	mixed regime (>500km ²)	1.41	1842.89	123.14	2077.41
2020	Ticino	Bellinzona	721245 / 117025	0.2	1517.00	1679	mixed regime (>500km ²)	4.27	1658.40	209.25	1339.14
2024	Rhône	Branson	573150 / 108300	13.0	3728.00	2235	mixed regime (>500km ²)	1.35	1249.40	133.83	1166.41
2029	Aare	Brigg, Aegerten	588220 / 219020	2.1	8249.00	1142	mixed regime (>500km ²)	6.73	1366.01	276.35	908.00
2030	Aare	Thun	613230 / 179280	6.9	2459.00	1746	mixed regime (>500km ²)	3.72	1604.05	176.90	1438.59
2033	Vorderrhein	Ilanz	735000 / 182030	1.8	774.00	2030	mixed regime (>500km ²)	2.28	1534.35	157.08	1340.76
2034	Broye	Payenne, Caserne d'aviation	561660 / 187320	0.0	416.00	715	pluvial inférieur	9.19	1186.40	322.34	564.59
2044	Thur	Andelfingen	693510 / 272500	0.0	1702.00	770	mixed regime (>500km ²)	8.25	1392.81	333.74	857.45
2053	Dranche	Martigny, Pont de Rossetan	570930 / 105200	11.3	676.00	2250	mixed regime (>500km ²)	1.40	1269.62	138.70	462.70
2056	Reuss	Seedorf	690085 / 193210	6.4	833.00	2013	mixed regime (>500km ²)	1.96	1681.87	150.85	1624.38
2063	Aare	Murgenthal	629530 / 235090	1.7	10059.00	1066	mixed regime (>500km ²)	7.04	1346.17	284.49	888.26
2070	Emme	Emmenmatt, nur Hauptstation	623610 / 200420	0.0	443.00	1065	nivo-pluvial préalpin	6.94	1539.26	300.29	835.36
2078	Poschiavino	Le Prese, stazione principale	803490 / 130520	4.0	168.00	2162	nival méridional	1.58	1324.78	175.84	1064.96
2084	Mucota	Ingenbohl	688230 / 206140	0.0	317.00	1363	nival de transition	5.45	1958.67	237.00	1915.23
2085	Aare	Hagneck	580680 / 211650	3.4	5112.00	1368	mixed regime (>500km ²)	5.61	1452.15	237.22	1068.53
2086	Brenno	Loderio	717770 / 137270	0.3	400.00	1815	nival méridional	3.68	1618.84	185.01	342.59
2087	Reuss	Andermatt	688120 / 166320	2.9	190.00	2284	b-glacio-nival	0.59	1709.03	116.01	1167.49
2091	Rhein	Rheinfelden, Messstation	627190 / 267840	0.8	34524.00	1068	mixed regime (>500km ²)	6.68	1351.54	281.92	935.92
2099	Limmat	Zürich, Unterhard	682055 / 249430	0.8	2174.00	1194	mixed regime (>500km ²)	6.28	1719.03	264.98	1353.24
2102	Sarner Aa	Sarnen	661460 / 194220	0.0	269.00	1281	downstream lake	5.99	1648.90	224.99	1167.84
2104	Linth	Weesen, Bläsi	725160 / 221380	1.6	1062.00	1584	mixed regime (>500km ²)	4.39	1785.64	221.45	1538.41
2105	Inn	St. Moritzbad	783910 / 150960	3.8	155.00	2399	b-glacio-nival	-0.33	1055.10	161.39	1145.54
2106	Birs	Münchenstein, Hofmatt	613570 / 263080	0.0	887.00	728	mixed regime (>500km ²)	8.53	1206.82	335.73	545.50
2109	Lätschine	Gsteig	633130 / 168200	13.5	381.00	2050	a-glacio-nival	2.11	1780.73	119.63	1580.50
2110	Reuss	Mühlau, Hünenberg	672520 / 230600	2.2	2902.00	1371	mixed regime (>500km ²)	5.42	1641.78	226.17	1399.39
2112	Sitter	Appenzell	749040 / 244220	0.1	74.40	1256	nival de transition	6.22	1896.65	345.94	1421.58
2117	Dranche de Bagnes	Le Châble, Villette	582550 / 103270	22.1	254.00	2609	b-glaciaire	-0.59	1274.15	118.82	254.59
2119	Sarine	Fribourg	579420 / 183670	0.2	1271.00	1247	mixed regime (>500km ²)	6.35	1420.49	276.29	975.93
2122	Birse	Moutier, La Charmue	595740 / 237010	0.0	186.00	921	nivo-pluvial jurassien	7.49	1371.76	333.62	520.67

T = Temperature, P = Precipitation, E = Evaporation, Q = Streamflow/Runoff



Table A3. Characteristics of all 184 catchments in the HYD-RESPONSES dataset (Part 2/5).

Catchment	Water name	Place	Lon / Lat EPSG:21781	Glaciation %	Area km ²	Avg. Height m asl	Regime Type	Yearly Avg. T °C	Yearly P mm	Yearly E mm	Yearly Q mm
2125	Lorze	Frauenhal	674715 / 229845	0.0	262.00	678	downstream lake	8.91	1427.56	309.43	911.18
2126	Murg	Wängi	714105 / 261720	0.0	80.20	652	pluvial inférieur	8.72	1282.82	340.64	693.21
2132	Töss	Neftenbach	691460 / 263820	0.0	343.00	658	pluvial inférieur	8.89	1331.52	339.46	701.10
2135	Aare	Bern, Schönbühl	600710 / 198000	5.8	2941.00	1596	mixed regime (>500km ²)	4.43	1542.51	196.01	1317.74
2139	Rheinthal Binnenskanal	St. Margrethen	767160 / 257780	0.0	175.00	710	artificial waterbody	9.01	1451.16	310.08	2038.65
2141	Albula	Tiefencastel	763420 / 170145	0.5	529.00	2128	mixed regime (>500km ²)	1.53	1018.61	159.38	904.27
2143	Rhein	Rekingen	667060 / 269230	0.2	14767.00	1131	mixed regime (>500km ²)	5.83	1296.20	276.20	945.75
2150	Landquart	Felsenbach	765365 / 204910	0.7	614.00	1797	mixed regime (>500km ²)	3.34	1289.45	188.82	1203.19
2151	Simme	Oberwil	600060 / 167090	2.4	344.00	1641	nival de transition	4.52	1536.17	215.10	1084.54
2152	Reuss	Luzern, Geissmatthütte	665330 / 211800	2.8	2254.00	1504	mixed regime (>500km ²)	4.72	1683.08	207.59	1526.87
2155	Emme	Wiler, Limpachmündung, nur Hauptstation	608220 / 223240	0.0	924.00	863	mixed regime (>500km ²)	7.80	1356.58	313.03	316.15
2159	Gürbe	Belp, Mülimatt	604810 / 192680	0.0	116.00	846	pluvial supérieur	8.05	1236.50	298.87	715.53
2160	Sarine	Broc, Château d'en bas	573520 / 161345	0.3	636.00	1500	mixed regime (>500km ²)	5.12	1500.63	248.29	1014.01
2161	Massa	Blatten bei Naters	643700 / 137290	56.5	196.00	2937	a-glaciaire	-2.89	2036.03	45.98	2433.50
2167	Tresa	Ponte Tresa, Rocchetta	709580 / 92145	0.0	609.00	803	mixed regime (>500km ²)	9.59	1789.28	351.80	1107.04
2170	Arve	Genève, Bout du Monde	501220 / 115120	5.1	1973.00	1370	mixed regime (>500km ²)	5.65	1505.42	249.36	1153.49
2174	Rhône	Chancy, Aux Ripes	486600 / 112340	6.6	10308.00	1569	mixed regime (>500km ²)	4.32	1324.91	216.70	1027.76
2176	Sihl	Zürich, Sihlhölzli	682145 / 246890	0.0	343.00	1045	nivo-pluvial préalpin	6.97	1787.58	294.48	621.39
2179	Sense	Thorishaus, Sensematt	593350 / 193020	0.0	351.00	1071	nivo-pluvial préalpin	7.22	1404.55	306.68	756.67
2181	Thur	Halden	733560 / 263180	0.0	1085.00	908	mixed regime (>500km ²)	7.61	1585.63	329.74	1082.92
2185	Plessur	Chur, nur Hauptstation	757975 / 191925	0.0	264.00	1868	nival alpin	3.42	1179.00	194.41	693.27
2187	Werdenberger Binnenskanal	Salez	756795 / 234005	0.0	183.00	1003	artificial waterbody	7.74	1547.48	279.64	1344.65
2199	Wiese	Basel	611800 / 269700	0.0	442.00	720	pluvial jurassien	10.67	1508.42	342.75	800.00
2200	Weisse Lütchine	Zweilütschinen	635310 / 164550	13.1	165.00	2165	a-glacio-nival	1.58	1767.24	112.23	1531.27
2202	Ergolz	Liestal	622270 / 259750	0.0	261.00	588	pluvial jurassien	9.55	1076.57	341.74	436.87
2203	Grande Eau	Aigle	563975 / 129825	0.8	132.00	1562	nival de transition	4.96	1617.15	240.72	1082.21
2205	Aare	Untersiggenthal, Stilli	659970 / 263180	1.4	17553.00	1064	mixed regime (>500km ²)	6.99	1416.13	279.19	984.66
2206	Melera	Melera (Valle Morobbia)	726988 / 114670	0.0	1.07	1423	nivo-pluvial méridional	5.88	1712.31	290.07	1297523.71
2210	Doubs	Ocourt	572530 / 244460	0.0	1275.00	952	mixed regime (>500km ²)	7.10	1499.13	346.76	790.06
2215	Saane	Laupen	584440 / 195300	0.1	1862.00	1137	mixed regime (>500km ²)	6.87	1373.00	288.00	866.85
2219	Simme	Oberried / Lenk	602630 / 141660	22.6	34.80	2347	b-glaciaire	0.92	1779.85	171.95	2130.36
2232	Allenbach	Adelboden	608710 / 148300	0.0	28.80	1863	nival alpin	3.64	1557.08	174.36	1332.39
2239	Spöl	Punt dal Gall	811020 / 167920	0.3	295.00	2389	nivo-glaciaire	-0.61	940.86	152.75	105.09
2243	Limmat	Baden, Limmatpromenade	665640 / 258690	0.7	2394.00	1131	mixed regime (>500km ²)	6.59	1662.82	272.41	1311.73
2244	Krummbach	Klusmatten	644500 / 119420	0.4	19.40	2271	nival méridional	1.35	1342.63	166.60	1232.18
2247	Doubs	Sortie du lac des Brenets	544560 / 214880	0.0	867.00	977	mixed regime (>500km ²)	6.41	1548.43	350.16	635.02
2251	Rotenbach	Plaffien, Schwyberg	587980 / 170590	0.0	1.69	1455	nival de transition	5.70	1688.19	296.97	1427822.37
2252	Schwindlibach	Plaffien, Schwyberg	588340 / 171015	0.0	1.38	1439	nival de transition	5.76	1662.14	296.97	832954.23
2256	Rosengbach	Pontresina	788810 / 151690	21.7	66.50	2704	a-glaciaire	-1.75	1137.41	119.24	1398.90
2262	Berninabach	Pontresina	789440 / 151320	14.4	107.00	2615	a-glacio-nival	-1.18	1203.87	131.81	1411.84
2263	Chamuerabach	La Punt-Chamues-ch	791430 / 160600	0.1	73.40	2548	nivo-glaciaire	-1.10	1011.37	145.82	930.92
2265	Inn	Tarasp	816800 / 185910	3.0	1581.00	2384	mixed regime (>500km ²)	-0.37	992.18	147.59	383.43
2268	Rhone	Gletsch	670810 / 157200	41.8	39.40	2710	a-glaciaire	-1.75	1937.62	75.90	2342.03
2269	Lonza	Blatten	629130 / 140910	24.7	77.40	2624	a-glaciaire	-1.28	1566.54	86.75	1924.12
2276	Grosstalbach	Isenthal	685500 / 196050	6.7	43.90	1819	nival alpin	3.28	1731.55	227.73	1270.99

T = Temperature, P = Precipitation, E = Evaporation, Q = Streamflow/Runoff



Table A4. Characteristics of all 184 catchments in the HYD-RESPONSES dataset (Part 3/5).

Catchment	Water name	Place	Lon / Lat EPSG:21781	Glaciation %	Area km ²	Avg. Height m asl	Regime Type	Yearly Avg. T °C	Yearly P mm	Yearly E mm	Yearly Q mm
2282	Sperbelgraben	Wasen, Kurzenetalp	630725 / 207270	0.0	0.56	1070	nivo-pluvial préalpin	7.06	1631.78	342.53	883404.51
2283	Rappengraben	Wasen, Riedbad	634340 / 207350	0.0	0.60	1142	nivo-pluvial préalpin	6.87	1656.81	355.40	1064734.56
2288	Rhein	Neuhäusen, Flurlingerbrücke	689145 / 281975	0.3	11930.00	1239	mixed regime (>500km ²)	4.59	1295.50	261.93	960.66
2289	Rhein	Basel, Rheinhalde	613400 / 267650	0.8	35878.00	1052	mixed regime (>500km ²)	6.78	1343.83	284.04	919.47
2290	Areuse	St-Sulpice	532980 / 195880	0.0	104.00	1110	nivo-pluvial jurassien	5.67	1500.18	344.81	1408.21
2299	Alpbach	Ersfeld, Bodenberg	688560 / 185120	19.7	20.70	2205	b-glaciaire	1.07	1669.66	171.48	2406.18
2300	Minster	Euthal, Rütli	704425 / 215310	0.0	59.10	1352	nival de transition	5.53	2115.46	259.83	1639.61
2303	Thur	Jonschwil, Mühlaus	723675 / 252720	0.0	493.00	1021	nivo-pluvial préalpin	6.93	1757.19	320.59	1285.82
2304	Ova dal Fuom	Zomez, Punt la Drossa	810560 / 170790	0.0	55.30	2327	nival alpin	-0.46	937.69	150.89	586.32
2305	Glatt	Herisau, Zellersmühle	737270 / 251290	0.0	16.70	829	pluvial supérieur	8.18	1491.95	329.49	1063.60
2307	Suze	Sonceboz	579810 / 227350	0.0	127.00	1036	nivo-pluvial jurassien	6.97	1332.88	340.21	1008.10
2308	Goldach	Goldach, Bleiche, nur Hauptstation	753190 / 261590	0.0	50.40	832	pluvial supérieur	8.33	1423.14	317.59	853.11
2312	Aach	Salmsach, Hungerbühl	744410 / 268400	0.0	47.40	467	pluvial inférieur	9.68	1019.41	335.09	488.00
2319	Ova da Chuozza	Zomez	804930 / 174830	0.0	27.00	2371	nivo-glaciaire	-0.47	919.61	150.80	888.70
2321	Cassarate	Pregassona	718010 / 97380	0.0	75.80	987	pluvio-nival méridional	8.52	1900.06	330.75	983.33
2327	Dischmabach	Davos, Kriegsmatte	786020 / 183370	0.7	42.90	2376	b-glacio-nival	0.15	1015.77	147.17	1242.21
2342	Salina	Brig	642220 / 129630	2.5	76.50	2014	nivo-glaciaire	2.53	1165.38	167.60	948.67
2343	Langete	Huttwil, Häberenbad	629560 / 219135	0.0	59.90	760	pluvial inférieur	8.14	1276.02	329.38	618.66
2346	Rhone	Brig	641340 / 129700	19.2	906.00	2339	mixed regime (>500km ²)	0.31	1630.34	103.68	1481.12
2347	Riale di Roggiasca	Roveredo, Bacio di compenso	733545 / 118160	0.0	8.12	1702	nivo-pluvial méridional	4.11	1684.56	288.12	1869.20
2349	Breggia	Chiasso, Ponte di Polenta	722315 / 78320	0.0	47.10	933	pluvio-nival méridional	8.58	1726.83	382.64	712.61
2351	Vispa	Visp	634050 / 125900	23.1	786.00	2648	mixed regime (>500km ²)	-0.92	1125.42	116.03	684.02
2352	Linh	Linhthal, Ausgleichsbecken KLL, nur Haupt	718285 / 197310	9.4	147.00	2085	a-glacio-nival	1.83	1874.45	169.98	925.43
2355	Landwasser	Davos, Frauenkirch	779640 / 181200	0.3	184.00	2224	nivo-glaciaire	0.97	1063.29	151.03	926.33
2356	Riale di Calneggia	Cavergno, Pontit	684970 / 135960	0.0	23.90	2003	nival méridional	3.08	1868.56	188.46	1922.63
2364	Ticino	Piotta	694610 / 152450	0.3	159.00	2071	nival méridional	2.16	1803.44	136.09	413.29
2366	Poschiavino	La Rösä	802120 / 142010	0.0	14.10	2285	nival méridional	0.86	1398.05	162.22	1189.26
2368	Maggia	Locarno, Solduno	703100 / 113860	0.3	927.00	1530	mixed regime (>500km ²)	5.63	1946.42	245.77	783.83
2369	Mentue	Yvonand, La Mauguettaz	545440 / 180875	0.0	105.00	675	pluvial jurassien	9.35	1081.13	328.32	457.37
2370	Doubs	Le Noirmont, La Goule	561430 / 231050	0.0	1047.00	977	mixed regime (>500km ²)	6.69	1534.75	348.30	795.29
2371	Orbe	Le Chenit, Frontière	501445 / 156305	0.0	45.90	1235	nivo-pluvial jurassien	6.42	1901.34	337.96	615.79
2372	Linh	Mollis, Linthbrücke	723985 / 217965	2.9	600.00	1743	mixed regime (>500km ²)	3.49	1848.95	197.67	1687.89
2374	Necker	Mogelberg, Auchsäge	727110 / 247290	0.0	88.10	956	nivo-pluvial préalpin	7.27	1718.29	338.15	1142.38
2378	Orbe	Orbe, Le Chalet	530080 / 175560	0.0	343.00	1139	nivo-pluvial jurassien	6.73	1692.73	341.81	1016.62
2386	Murg	Frauenfeld	709540 / 269660	0.0	213.00	597	pluvial inférieur	8.98	1178.35	343.21	567.47
2387	Hinterhein	Fürstenu	755570 / 175730	0.6	1577.00	2127	mixed regime (>500km ²)	1.47	1147.93	165.74	767.37
2403	Inn	Cmuos-chel, nur Hauptstation	797700 / 168170	5.2	733.00	2456	mixed regime (>500km ²)	-0.66	1007.10	146.31	212.71
2409	Emme	Eggwil, Heidbüel	627910 / 191180	0.0	124.00	1281	nivo-pluvial préalpin	6.10	1604.24	270.21	1061.40
2410	Liechtensteiner Binnenkanal	Ruggell	757750 / 234590	0.0	116.00	853	artificial waterbody	8.58	1286.29	264.96	1321.13
2412	Sionge	Vuippens, Château	572420 / 167540	0.0	43.40	865	nivo-pluvial préalpin	8.10	1298.00	302.73	802.84
2414	Rietholz	Mosnang, Rietholz	718840 / 248440	0.0	3.19	794	pluvial supérieur	8.13	1476.78	336.69	1006909.39
2415	Glatt	Rheinsfelden	678040 / 269720	0.0	417.00	503	downstream lake	9.70	1165.36	340.63	590.10
2416	Aabach	Hitzkirch, Richensee	661390 / 230220	0.0	73.30	581	downstream lake	9.46	1163.00	317.37	535.90
2417	Suhre	Oberkirch	651320 / 223140	0.0	75.60	583	downstream lake	9.39	1139.68	312.72	510.78
2418	Julia	Tiefencastel	763570 / 169910	0.2	325.00	2196	nivo-glaciaire	1.10	1058.77	161.39	97.09
2419	Rhone	Rekingen	661910 / 146780	11.8	214.00	2305	a-glacio-nival	0.30	1814.00	105.51	1424.61
2420	Moesa	Lumino, Sassello	724765 / 120360	0.1	472.00	1667	nivo-pluvial méridional	3.98	1619.63	234.73	1339.42

T = Temperature, P = Precipitation, E = Evaporation, Q = Streamflow/Runoff



Table A5. Characteristics of all 184 catchments in the HYD-RESPONSES dataset (Part 4/5).

Catchment	Water name	Place	Lon / Lat EPSG:21781	Glaciation %	Area km ²	Avg. Height m asl	Regime Type	Yearly Avg. T °C	Yearly P mm	Yearly E mm	Yearly Q mm
2426	Siez	Mels	750410 / 212510	0.1	106.00	1803	nival alpin	3.55	1578.39	217.42	640.88
2430	Rein da Sunnvitg	Sunnvítg, Encardens	718810 / 167690	1.7	21.80	2457	b-glacio-nival	-0.15	1581.92	160.82	2183.90
2432	Venoge	Ecublens, Les Bois	532040 / 154160	0.0	228.00	686	nivo-pluvial jurassien	9.62	1148.17	332.99	539.44
2433	Aubonne	Allaman, Le Coulet	520720 / 147410	0.0	105.00	952	nivo-pluvial jurassien	8.21	1444.62	340.37	1587.98
2434	Dinnern	Oltén, Hammermühle	634330 / 244480	0.0	234.00	711	pluvial jurassien	8.50	1210.83	334.79	437.11
2436	Chli Schliere	Alpnach, Chlich Erti	663800 / 195770	0.0	21.60	1345	nivo-pluvial préalpin	5.96	1876.39	271.62	966.44
2437	Parinbot	Ecublens, Eschiens	552060 / 161650	0.0	6.92	716	pluvial jurassien	9.50	1182.10	311.77	717260.34
2450	Wigger	Zofingen	637580 / 237080	0.0	366.00	656	pluvial inférieur	8.80	1182.26	328.47	461.60
2457	Aare	Ringgenberg, Goldswil	633730 / 171510	12.1	1138.00	1951	mixed regime (>500km ²)	2.47	1761.77	138.78	1715.63
2458	Seyon	Valangin	559370 / 206810	0.0	112.00	978	nivo-pluvial jurassien	7.54	1292.29	350.00	214.91
2461	Magliasina	Magliaso, Ponte	711620 / 93290	0.0	34.40	926	pluvio-nival méridional	8.91	1938.53	357.01	1117.90
2468	Sitter	St. Gallen, Bruggen/Au	742540 / 253230	0.0	261.00	1042	nivo-pluvial préalpin	7.22	1722.67	343.20	1208.91
2471	Murg	Murgenthal, Walliswil	629340 / 233555	0.0	183.00	653	pluvial inférieur	8.60	1191.59	333.34	556.21
2473	Rhein	Diepoldskau, Rietbrücke	766280 / 250360	0.6	6299.00	1771	mixed regime (>500km ²)	3.17	1327.19	193.52	1163.69
2474	Calancasca	Buseno	729440 / 127180	0.2	121.00	1931	nival méridional	2.65	1673.78	227.69	1113.07
2475	Maggia	Bignasco, Ponte nuovo	690040 / 132550	0.9	316.00	1879	nival méridional	3.67	1939.62	187.23	415.67
2477	Lotze	Zug, Letzi	680600 / 226070	0.0	100.00	818	downstream lake	8.15	1560.20	295.43	925.59
2478	Birse	Soyhières, Bois du Treuil	596780 / 249070	0.0	569.00	805	nivo-pluvial jurassien	8.06	1265.37	334.76	580.60
2480	Areuse	Boudry	554350 / 199940	0.0	378.00	1077	nivo-pluvial jurassien	6.27	1464.77	347.62	906.66
2481	Engelberger Aa	Buchs, Flugplatz	673555 / 202870	2.5	228.00	1609	b-glacio-nival	4.30	1693.58	196.94	1705.73
2485	Allaine	Boncourt, Frontière	567830 / 261200	0.0	212.00	562	pluvial jurassien	9.54	1108.82	343.10	464.95
2486	Veveyse	Vevey, Copet	554675 / 146565	0.0	64.50	1098	nivo-pluvial préalpin	7.37	1497.99	307.89	955.88
2487	Kleine Emme	Werthenstein, Chappelboden	647870 / 209510	0.0	311.00	1167	nivo-pluvial préalpin	6.61	1695.60	279.00	1095.28
2488	Simme	Latterbach	610680 / 167840	1.5	563.00	1594	nival de transition	4.79	1506.56	225.96	342.76
2490	Allondon	Dardagny, Les Granges	488880 / 119460	0.0	119.00	760	nivo-pluvial jurassien	10.64	1372.60	326.46	854.70
2491	Schächen	Burglen, Galgenwäldli, nur Hauptstation	692480 / 191800	1.5	108.00	1728	nivo-glaciaire	3.55	1854.00	188.20	1397.24
2493	Promenthouse	Gland, Route Suisse	510080 / 140080	0.0	120.00	1027	nivo-pluvial jurassien	7.73	1577.83	338.92	430.80
2494	Ticino	Pollegio, Campagna	716120 / 135330	0.2	444.00	1796	nival méridional	3.85	1710.59	173.72	1438.77
2497	Luthern	Nebikon	640560 / 226740	0.0	105.00	749	pluvial inférieur	8.31	1268.69	334.87	429.99
2498	Glennet	Castrisch	735330 / 181790	1.1	381.00	2022	nivo-glaciaire	2.11	1307.02	168.97	734.66
2500	Worbte	Ittigen	603005 / 202455	0.0	67.10	666	pluvial inférieur	8.72	1174.24	317.69	475.10
2602	Rhein	Domat/Emm	753890 / 189370	0.9	3229.00	2013	mixed regime (>500km ²)	2.19	1277.76	168.28	1122.84
2603	Ilfis	Langnau	627320 / 198600	0.0	187.00	1039	nivo-pluvial préalpin	7.05	1619.21	318.70	882.14
2604	Biber	Biberbrugg	697240 / 223280	0.0	31.90	1003	nivo-pluvial préalpin	7.00	1789.15	287.37	1085.77
2605	Verzasca	Lavertezzo, Campiò	708420 / 122920	0.0	185.00	1651	nivo-pluvial méridional	5.11	2013.18	260.43	1846.37
2606	Rhône	Genève, Halle de l'Ile	499800 / 117850	7.2	8000.00	1658	mixed regime (>500km ²)	4.08	1286.36	204.12	996.79
2607	Goneri	Oberwald	670467 / 153932	4.0	38.50	2383	b-glacio-nival	0.07	1976.16	121.82	2011.50
2608	Sellenbodenbach	Neuenkirch	658530 / 218290	0.0	10.40	608	pluvial inférieur	9.33	1193.97	305.25	637.12

T = Temperature, P = Precipitation, E = Evaporation, Q = Streamflow/Runoff



Table A6. Characteristics of all 184 catchments in the HYD-RESPONSES dataset (Part 5/5).

Catchment	Water name	Place	Lon / Lat EPSG:21781	Glaciation %	Area km ²	Avg. Height m asl	Regime Type	Yearly Avg. T °C	Yearly P mm	Yearly E mm	Yearly Q mm
2609	Alp	Einsiedeln	698640 / 223020	0.0	46.70	1157	nivo-pluvial préalpin	6.35	1939.89	279.80	1459.07
2610	Scheulte	Vicques	599485 / 244150	0.0	72.70	792	nivo-pluvial jurassien	8.20	1260.81	333.18	635.64
2612	Riale di Pincascia	Lavertezzo	708060 / 123950	0.0	44.50	1705	nivo-pluvial méridional	4.89	1978.57	277.65	1911.93
2617	Rom	Mustair	830800 / 168700	0.0	128.00	2184	nival alpin	1.03	844.68	158.63	577.25
2620	Mera	Soglio	760770 / 133450	7.4	177.00	2173	b-glacio-nival	0.95	1333.42	191.09	361.81
2629	Vedeggio	Agno, stazione principale	714110 / 95680	0.0	99.90	921	pluvio-nival méridional	8.87	1904.96	334.27	656.21
2630	Sionne	Sion	594400 / 119900	0.0	27.60	1577	nival alpin	5.35	1355.03	186.55	224.58
2631	Hinterrhein	Hinterrhein, Schiessplatz	733706 / 153945	9.1	41.50	2430	a-glacio-nival	-0.38	1704.08	164.40	799.71
2634	Kleine Emme	Emmen	663700 / 213630	0.0	478.00	1054	nivo-pluvial préalpin	7.15	1610.61	284.17	994.18
2635	Grossbach	Einsiedeln, Gross	700710 / 218125	0.0	8.95	1283	nivo-pluvial préalpin	5.90	1952.69	299.45	1387.71
2640	Some	Delémont, Pré-Guillaume	593380 / 245940	0.0	214.00	779	nivo-pluvial jurassien	8.20	1233.60	335.80	603.72
2646	Kander	Emdthal	617790 / 168400	5.1	487.00	1860	b-glacio-nival	3.38	1486.71	167.85	1305.44

T = Temperature, P = Precipitation, E = Evaporation, Q = Streamflow/Runoff



615 References

- Apurv, T. and Cai, X.: Drought Propagation in Contiguous U.S. Watersheds: A Process-Based Understanding of the Role of Climate and Watershed Properties, *Water Resources Research*, 56, e2020WR027755, <https://doi.org/10.1029/2020WR027755>, <https://onlinelibrary.wiley.com/doi/pdf/10.1029/2020WR027755>, 2020.
- Apurv, T., Sivapalan, M., and Cai, X.: Understanding the Role of Climate Characteristics in Drought Propagation, *Water Resources Research*, 53, 9304–9329, <https://doi.org/10.1002/2017WR021445>, [eprint: https://onlinelibrary.wiley.com/doi/pdf/10.1002/2017WR021445](https://onlinelibrary.wiley.com/doi/pdf/10.1002/2017WR021445), 2017.
- 620 Aschwanden, H.: Die Niedrigwasserabflussmenge Q347 – Bestimmung und Abschätzung in alpinen schweizerischen Einzugsgebieten., Tech. Rep. 18, Bern, 1992.
- Aschwanden, H. and Kan, C.: Die Abflussmenge Q347 – eine Standortbestimmung., Tech. Rep. 27, Bern, 1999.
- Aschwanden, H. and Weingartner, R.: Die Abflussregimes der Schweiz., Tech. Rep. 65, Geographisches Institut der Universität Bern (GIUB), Bern, <https://boris.unibe.ch/133660/>, 1985.
- 625 Avanzi, F., Munerol, F., Milelli, M., Gabellani, S., Massari, C., Girotto, M., Cremonese, E., Galvagno, M., Bruno, G., Morra di Cella, U., Rossi, L., Altamura, M., and Ferraris, L.: Winter snow deficit was a harbinger of summer 2022 socio-hydrologic drought in the Po Basin, Italy, *Commun Earth Environ*, 5, 1–12, <https://doi.org/10.1038/s43247-024-01222-z>, publisher: Nature Publishing Group, 2024.
- Bachmair, S., Stahl, K., Collins, K., Hannaford, J., Acreman, M., Svoboda, M., Knutson, C., Smith, K. H., Wall, N., Fuchs, B., Crossman, N. D., and Overton, I. C.: Drought indicators revisited: the need for a wider consideration of environment and society, *WIREs Water*, 3, 516–536, <https://doi.org/10.1002/wat2.1154>, [eprint: https://onlinelibrary.wiley.com/doi/pdf/10.1002/wat2.1154](https://onlinelibrary.wiley.com/doi/pdf/10.1002/wat2.1154), 2016.
- 630 Bachmair, S., Tanguy, M., Hannaford, J., and Stahl, K.: How well do meteorological indicators represent agricultural and forest drought across Europe?, *Environ. Res. Lett.*, 13, 034042, <https://doi.org/10.1088/1748-9326/aaafda>, publisher: IOP Publishing, 2018.
- Baez-Villanueva, O. M., Zambrano-Bigiarini, M., Miralles, D. G., Beck, H. E., Siegmund, J. F., Alvarez-Garretón, C., Verbist, K., Garreaud, R., Boisier, J. P., and Galleguillos, M.: On the timescale of drought indices for monitoring streamflow drought considering catchment hydrological regimes, *Hydrology and Earth System Sciences*, 28, 1415–1439, <https://doi.org/10.5194/hess-28-1415-2024>, publisher: Copernicus GmbH, 2024.
- 635 BAFU: Hitze und Trockenheit im Sommer 2015. Auswirkungen auf Mensch und Umwelt. Bundesamt für Umwelt BAFU, Bern. Umwelt-Zustand Nr. 1629: 108 S., Tech. rep., 2016.
- 640 BAFU: Nationale Grundwasserbeobachtung NAQUA, <https://www.bafu.admin.ch/bafu/de/home/themen/thema-wasser/wasser-fachinformationen/zustand-der-gewaesser/zustand-des-grundwassers/nationale-grundwasserbeobachtung-naqua.html>, 2019.
- BAFU: Trockenheit: Bundesrat will nationales System zur Früherkennung und Warnung, <https://www.bafu.admin.ch/bafu/de/home/dokumentation/medienmitteilungen/anzeige-nsb-unter-medienmitteilungen.msg-id-88854.html>, 2022.
- BAFU: Nationale Beobachtung Oberflächengewässerqualität (NAWA), <https://www.bafu.admin.ch/bafu/de/home/themen/thema-wasser/wasser-daten-indikatoren-und-karten/wasser-messnetze/nationale-beobachtung-oberflaechengewaesserqualitaet-nawa-.html>, 2023.
- 645 BAFU: Stationsbericht Niedrigwasserstatistik - Leitfaden, <https://www.bafu.admin.ch/dam/bafu/de/dokumente/hydrologie/fachinfo-daten/leitfaden-stationsberichte-niedrigwasserstatistik-bafu.pdf.download.pdf/leitfaden-stationsberichte-niedrigwasserstatistik-bafu.pdf>, 2024.
- BAFU et al. (Hrsg.): Hitze und Trockenheit im Sommer 2018. Auswirkungen auf Mensch und Umwelt. Bundesamt für Umwelt, Bern. Umwelt-Zustand Nr. 1909: 91 S., Tech. rep., 2019.
- 650 BAFU (Hrsg.): Auswirkungen des Klimawandels auf die Schweizer Gewässer. Hydrologie, Gewässerökologie und Wasserwirtschaft. Bundesamt für Umwelt BAFU, Bern. Umwelt-Wissen Nr. 2101: 134 S., Tech. rep., 2021.



- BAFU (Hrsg.): Die biogeographischen Regionen der Schweiz. 1. aktualisierte Auflage 2022. Erstausgabe 2001. Bundesamt für Umwelt, Bern, Umwelt-Wissen Nr. 2214: p.28, Tech. rep., Bundesamt für Umwelt, https://www.bafu.admin.ch/dam/bafu/de/dokumente/landschaft/uw-umwelt-wissen/die_biogeographischenregionenderschweiz.pdf.download.pdf/die_biogeographischenregionenderschweiz.pdf, 2022.
- 655 BAFU (Hrsg.): Hydrologisches Jahrbuch der Schweiz 2022. Abfluss, Wasserstand und Wasserqualität der Schweizer Gewässer., Tech. rep., Bundesamt für Umwelt, Ittigen, Bern, https://www.bafu.admin.ch/dam/bafu/de/dokumente/hydrologie/uz-umwelt-zustand/hydrologisches-jahrbuch-2022.pdf.download.pdf/de_BAFU_UZ_2215_Hydrologisches_Jahrbuch_2022_bf.pdf, 2023.
- Baker, D. B., Richards, R. P., Loftus, T. T., and Kramer, J. W.: A New Flashiness Index: Characteristics and Applications to Midwestern Rivers and Streams, *JAWRA Journal of the American Water Resources Association*, 40, 503–522, <https://doi.org/10.1111/j.1752-1688.2004.tb01046.x>, [eprint: https://onlinelibrary.wiley.com/doi/pdf/10.1111/j.1752-1688.2004.tb01046.x](https://onlinelibrary.wiley.com/doi/pdf/10.1111/j.1752-1688.2004.tb01046.x), 2004.
- 660 Barker, L. J., Hannaford, J., Chiverton, A., and Svensson, C.: From meteorological to hydrological drought using standardised indicators, *Hydrology and Earth System Sciences*, 20, 2483–2505, <https://doi.org/10.5194/hess-20-2483-2016>, publisher: Copernicus GmbH, 2016.
- Baston, D.: exactextractr: Fast Extraction from Raster Datasets using Polygons. R package version 0.10.0, <https://cran.r-project.org/web/packages/exactextractr/index.html>, 2023.
- 665 Bevacqua, E., De Michele, C., Manning, C., Couasnon, A., Ribeiro, A. F. S., Ramos, A. M., Vignotto, E., Bastos, A., Blesić, S., Durante, F., Hillier, J., Oliveira, S. C., Pinto, J. G., Ragno, E., Rivoire, P., Saunders, K., van der Wiel, K., Wu, W., Zhang, T., and Zscheischler, J.: Guidelines for Studying Diverse Types of Compound Weather and Climate Events, *Earth’s Future*, 9, e2021EF002 340, <https://doi.org/10.1029/2021EF002340>, [eprint: https://onlinelibrary.wiley.com/doi/pdf/10.1029/2021EF002340](https://onlinelibrary.wiley.com/doi/pdf/10.1029/2021EF002340), 2021.
- Bloomfield, J. P., Gong, M., Marchant, B. P., Coxon, G., and Addor, N.: How is Baseflow Index (BFI) impacted by water resource management practices?, *Hydrology and Earth System Sciences*, 25, 5355–5379, <https://doi.org/10.5194/hess-25-5355-2021>, publisher: Copernicus GmbH, 2021.
- 670 BLW, B. f. L.: Bodeneignungskarte der Schweiz, <https://www.blw.admin.ch/blw/de/home/politik/datenmanagement/geografisches-informationssystem-gis/bodeneignungskarte.html>, 2022.
- Brocca, L., Barbetta, S., Camici, S., Ciabatta, L., Dari, J., Filippucci, P., Massari, C., Modanesi, S., Tarpanelli, A., Bonaccorsi, B., Mosaffa, H., Wagner, W., Vreugdenhil, M., Quast, R., Alfieri, L., Gabellani, S., Avanzi, F., Rains, D., Miralles, D. G., Mantovani, S., Briese, C., Domeneghetti, A., Jacob, A., Castelli, M., Camps-Valls, G., Volden, E., and Fernandez, D.: A Digital Twin of the terrestrial water cycle: a glimpse into the future through high-resolution Earth observations, *Front. Sci.*, 1, <https://doi.org/10.3389/fsci.2023.1190191>, publisher: Frontiers, 2024.
- 675 Brunner, M. I. and Chartier-Rescan, C.: Drought Spatial Extent and Dependence Increase During Drought Propagation From the Atmosphere to the Hydrosphere, *Geophysical Research Letters*, 51, e2023GL107 918, <https://doi.org/10.1029/2023GL107918>, [eprint: https://onlinelibrary.wiley.com/doi/pdf/10.1029/2023GL107918](https://onlinelibrary.wiley.com/doi/pdf/10.1029/2023GL107918), 2024.
- Brunner, M. I., Björnson Gurung, A., Zappa, M., Zekollari, H., Farinotti, D., and Stähli, M.: Present and future water scarcity in Switzerland: Potential for alleviation through reservoirs and lakes, *Science of The Total Environment*, 666, 1033–1047, <https://doi.org/10.1016/j.scitotenv.2019.02.169>, 2019a.
- 685 Brunner, M. I., Liechti, K., and Zappa, M.: Extremeness of recent drought events in Switzerland: dependence on variable and return period choice, *Natural Hazards and Earth System Sciences*, 19, 2311–2323, <https://doi.org/10.5194/nhess-19-2311-2019>, publisher: Copernicus GmbH, 2019b.
- Brunner, M. I., Slater, L., Tallaksen, L. M., and Clark, M.: Challenges in modeling and predicting floods and droughts: A review, *WIREs Water*, 8, e1520, <https://doi.org/10.1002/wat2.1520>, [eprint: https://onlinelibrary.wiley.com/doi/pdf/10.1002/wat2.1520](https://onlinelibrary.wiley.com/doi/pdf/10.1002/wat2.1520), 2021.



- 690 Brunner, M. I., Van Loon, A. F., and Stahl, K.: Moderate and Severe Hydrological Droughts in Europe Differ in Their Hydrometeorological Drivers, *Water Resources Research*, 58, e2022WR032871, <https://doi.org/10.1029/2022WR032871>, _eprint: <https://onlinelibrary.wiley.com/doi/pdf/10.1029/2022WR032871>, 2022.
- Brunner, M. I., Götte, J., Schlemper, C., and Van Loon, A. F.: Hydrological Drought Generation Processes and Severity Are Changing in the Alps, *Geophysical Research Letters*, 50, e2022GL101776, <https://doi.org/10.1029/2022GL101776>, _eprint: <https://onlinelibrary.wiley.com/doi/pdf/10.1029/2022GL101776>, 2023.
- 695 BUWAL, BWG, MeteoSchweiz: Auswirkungen des Hitzesommers 2003 auf die Gewässer. Schriftenreihe Umwelt Nr. 369. Bern: Bundesamt für Umwelt, Wald und Landschaft, 174 S., Tech. rep., 2004.
- Calanca, P.: Climate change and drought occurrence in the Alpine region: How severe are becoming the extremes?, *Global and Planetary Change*, 57, 151–160, <https://doi.org/10.1016/j.gloplacha.2006.11.001>, 2007.
- 700 Cammalleri, C., Barbosa, P., and Vogt, J. V.: Analysing the Relationship between Multiple-Timescale SPI and GRACE Terrestrial Water Storage in the Framework of Drought Monitoring, *Water*, 11, 1672, <https://doi.org/10.3390/w11081672>, number: 8 Publisher: Multidisciplinary Digital Publishing Institute, 2019.
- CH2018: CH2018 – Climate Scenarios for Switzerland, Technical Report, National Centre for Climate Services, Zurich, 271 pp. ISBN: 978-3-9525031-4-0., Tech. rep., 2018.
- 705 Clerc-Schwarzenbach, F., Selleri, G., Neri, M., Toth, E., van Meerveld, I., and Seibert, J.: Large-sample hydrology – a few camels or a whole caravan?, *Hydrology and Earth System Sciences*, 28, 4219–4237, <https://doi.org/10.5194/hess-28-4219-2024>, publisher: Copernicus GmbH, 2024.
- Dalla Torre, D., Di Marco, N., Menapace, A., Avesani, D., Righetti, M., and Majone, B.: Suitability of ERA5-Land re-analysis dataset for hydrological modelling in the Alpine region, *Journal of Hydrology: Regional Studies*, 52, 101718, <https://doi.org/10.1016/j.ejrh.2024.101718>, 2024.
- 710 Das, B. C., Islam, A., and Sarkar, B.: Drainage Basin Shape Indices to Understanding Channel Hydraulics, *Water Resour Manage*, 36, 2523–2547, <https://doi.org/10.1007/s11269-022-03121-4>, 2022.
- de Jager, A., Corbane, C., and Szabo, F.: Recent Developments in Some Long-Term Drought Drivers, *Climate*, 10, 31, <https://doi.org/10.3390/cli10030031>, number: 3 Publisher: Multidisciplinary Digital Publishing Institute, 2022.
- 715 Ding, Y., Gong, X., Xing, Z., Cai, H., Zhou, Z., Zhang, D., Sun, P., and Shi, H.: Attribution of meteorological, hydrological and agricultural drought propagation in different climatic regions of China, *Agricultural Water Management*, 255, 106996, <https://doi.org/10.1016/j.agwat.2021.106996>, 2021.
- Dingman, S. L.: Drainage density and streamflow: A closer look, *Water Resources Research*, 14, 1183–1187, <https://doi.org/10.1029/WR014i006p01183>, _eprint: <https://onlinelibrary.wiley.com/doi/pdf/10.1029/WR014i006p01183>, 1978.
- 720 Eekhout, J. P. C., Hunink, J. E., Terink, W., and de Vente, J.: Why increased extreme precipitation under climate change negatively affects water security, *Hydrology and Earth System Sciences*, 22, 5935–5946, <https://doi.org/10.5194/hess-22-5935-2018>, publisher: Copernicus GmbH, 2018.
- European Commission: Standardized Precipitation Index (SPI). EDO Indicator Factsheet. European Drought Observatory (EDO)., https://edo.jrc.ec.europa.eu/documents/factsheets/factsheet_spi.pdf, 2020.
- 725 Floriancic, M. G., Berghuijs, W. R., Jonas, T., Kirchner, J. W., and Molnar, P.: Effects of climate anomalies on warm-season low flows in Switzerland, *Hydrology and Earth System Sciences*, 24, 5423–5438, <https://doi.org/10.5194/hess-24-5423-2020>, publisher: Copernicus GmbH, 2020.



- Floriancic, M. G., Spies, D., van Meerveld, I. H. J., and Molnar, P.: A multi-scale study of the dominant catchment characteristics impacting low-flow metrics, *Hydrological Processes*, 36, e14462, <https://doi.org/10.1002/hyp.14462>, _eprint: <https://onlinelibrary.wiley.com/doi/pdf/10.1002/hyp.14462>, 2022.
- Frei, C.: Interpolation of temperature in a mountainous region using nonlinear profiles and non-Euclidean distances, *International Journal of Climatology*, 34, 1585–1605, <https://doi.org/10.1002/joc.3786>, _eprint: <https://onlinelibrary.wiley.com/doi/pdf/10.1002/joc.3786>, 2014.
- Frei, C. and Schär, C.: A precipitation climatology of the Alps from high-resolution rain-gauge observations, *International Journal of Climatology*, 18, 873–900, [https://doi.org/10.1002/\(SICI\)1097-0088\(19980630\)18:8<873::AID-JOC255>3.0.CO;2-9](https://doi.org/10.1002/(SICI)1097-0088(19980630)18:8<873::AID-JOC255>3.0.CO;2-9), _eprint: <https://onlinelibrary.wiley.com/doi/pdf/10.1002/%28SICI%291097-0088%2819980630%2918%3A8%3C873%3A%3AAID-JOC255%3E3.0.CO%3B2-9>, 1998.
- Gudmundsson, L. and Stagge, J. H.: SCI: Standardized Climate Indices such as SPI, SRI or SPEIR package version 1.0-2., 2016.
- Guo, Y., Zhang, Y., Zhang, L., and Wang, Z.: Regionalization of hydrological modeling for predicting streamflow in ungauged catchments: A comprehensive review, *WIREs Water*, 8, e1487, <https://doi.org/10.1002/wat2.1487>, _eprint: <https://onlinelibrary.wiley.com/doi/pdf/10.1002/wat2.1487>, 2021.
- Haile, G. G., Tang, Q., Li, W., Liu, X., and Zhang, X.: Drought: Progress in broadening its understanding, *WIREs Water*, 7, e1407, <https://doi.org/10.1002/wat2.1407>, _eprint: <https://onlinelibrary.wiley.com/doi/pdf/10.1002/wat2.1407>, 2020.
- Hao, Z. and Singh, V. P.: Drought characterization from a multivariate perspective: A review, *Journal of Hydrology*, 527, 668–678, <https://doi.org/10.1016/j.jhydrol.2015.05.031>, 2015.
- Haslinger, K., Koffler, D., Schöner, W., and Laaha, G.: Exploring the link between meteorological drought and streamflow: Effects of climate-catchment interaction, *Water Resources Research*, 50, 2468–2487, <https://doi.org/10.1002/2013WR015051>, _eprint: <https://onlinelibrary.wiley.com/doi/pdf/10.1002/2013WR015051>, 2014.
- Henne, P. D., Bigalke, M., Büntgen, U., Colombaroli, D., Conedera, M., Feller, U., Frank, D., Fuhrer, J., Grosjean, M., Heiri, O., Luterbacher, J., Mestrot, A., Rigling, A., Rössler, O., Rohr, C., Rutishauser, T., Schwikowski, M., Stampfli, A., Szidat, S., Theurillat, J.-P., Weingartner, R., Wilcke, W., and Tinner, W.: An empirical perspective for understanding climate change impacts in Switzerland, *Reg Environ Change*, 18, 205–221, <https://doi.org/10.1007/s10113-017-1182-9>, 2018.
- Hersbach, H., Bell, B., Berrisford, P., Hirahara, S., Horányi, A., Muñoz-Sabater, J., Nicolas, J., Peubey, C., Radu, R., Schepers, D., Simmons, A., Soci, C., Abdalla, S., Abellan, X., Balsamo, G., Bechtold, P., Biavati, G., Bidlot, J., Bonavita, M., De Chiara, G., Dahlgren, P., Dee, D., Diamantakis, M., Dragani, R., Flemming, J., Forbes, R., Fuentes, M., Geer, A., Haimberger, L., Healy, S., Hogan, R. J., Hólm, E., Janisková, M., Keeley, S., Laloyaux, P., Lopez, P., Lupu, C., Radnoti, G., de Rosnay, P., Rozum, I., Vamborg, F., Villaume, S., and Thépaut, J.-N.: The ERA5 global reanalysis, *Quarterly Journal of the Royal Meteorological Society*, 146, 1999–2049, <https://doi.org/10.1002/qj.3803>, _eprint: <https://onlinelibrary.wiley.com/doi/pdf/10.1002/qj.3803>, 2020.
- Hijmans, R.: terra: Spatial Data Analysis. R package version 1.7-29., <https://cran.r-project.org/web/packages/terra/>, 2023.
- Hisdal, H. and Tallaksen, L. M.: Drought event definition. Technical Report to the ARIDE project No. 6. Department of Geophysics, University of Oslo., Tech. rep., 2000.
- Höge, M., Kauzlaric, M., Siber, R., Schönenberger, U., Horton, P., Schwanbeck, J., Floriancic, M. G., Viviroli, D., Wilhelm, S., Sikorska-Senoner, A. E., Addor, N., Brunner, M., Pool, S., Zappa, M., and Fenicia, F.: CAMELS-CH: hydro-meteorological time series and landscape attributes for 331 catchments in hydrologic Switzerland, *Earth System Science Data*, 15, 5755–5784, <https://doi.org/10.5194/essd-15-5755-2023>, publisher: Copernicus GmbH, 2023a.



- 765 Höge, M., Kauzlaric, M., Siber, R., Schönenberger, U., Horton, P., Schwanbeck, J., Floriancic, M. G., Viviroli, D., Wilhelm, S., Sikorska-Senoner, A. E., Addor, N., Brunner, M., Pool, S., Zappa, M., and Fenicia, F.: Catchment attributes and hydro-meteorological time series for large-sample studies across hydrologic Switzerland (CAMELS-CH), <https://doi.org/10.5281/zenodo.10354485>, 2023b.
- Imfeld, N., Stucki, P., Brönnimann, S., Bürgi, M., Calanca, P., Holzkämper, A., Isotta, F., Nussbaumer, S. U., Scherrer, S., Staub, K., Vicedo-Cabrera, A., Wohlgemuth, T., and Zumbühl, H. J.: 2022: Ein ziemlich normaler zukünftiger Sommer, *Geographica Bernensia*, G100, 1–3, <https://doi.org/10.4480/GB2022.G100>, publisher: Geographisches Institut Universität Bern, 2022.
- 770 Jehn, F. U., Bestian, K., Breuer, L., Kraft, P., and Houska, T.: Using hydrological and climatic catchment clusters to explore drivers of catchment behavior, *Hydrology and Earth System Sciences*, 24, 1081–1100, <https://doi.org/10.5194/hess-24-1081-2020>, publisher: Copernicus GmbH, 2020.
- Kchouk, S., Melsen, L. A., Walker, D. W., and van Oel, P. R.: A geography of drought indices: mismatch between indicators of drought and its impacts on water and food securities, *Natural Hazards and Earth System Sciences*, 22, 323–344, <https://doi.org/10.5194/nhess-22-323-2022>, publisher: Copernicus GmbH, 2022.
- 775 Koehler, J., Dietz, A. J., Zellner, P., Baumhoer, C. A., Dirscherl, M., Cattani, L., Vlahović, , Alasawedah, M. H., Mayer, K., Haslinger, K., Bertoldi, G., Jacob, A., and Kuenzer, C.: Drought in Northern Italy: Long Earth Observation Time Series Reveal Snow Line Elevation to Be Several Hundred Meters Above Long-Term Average in 2022, *Remote Sensing*, 14, 6091, <https://doi.org/10.3390/rs14236091>, number: 23 Publisher: Multidisciplinary Digital Publishing Institute, 2022.
- 780 Kotlarski, S., Gobiet, A., Morin, S., Olefs, M., Rajczak, J., and Samacoïts, R.: 21st Century alpine climate change, *Clim Dyn*, 60, 65–86, <https://doi.org/10.1007/s00382-022-06303-3>, 2023.
- Kratzert, F., Klotz, D., Brenner, C., Schulz, K., and Herrnegger, M.: Rainfall–runoff modelling using Long Short-Term Memory (LSTM) networks, *Hydrology and Earth System Sciences*, 22, 6005–6022, <https://doi.org/10.5194/hess-22-6005-2018>, publisher: Copernicus GmbH, 2018.
- 785 Kratzert, F., Nearing, G., Addor, N., Erickson, T., Gauch, M., Gilon, O., Gudmundsson, L., Hassidim, A., Klotz, D., Nevo, S., Shalev, G., and Matias, Y.: Caravan - A global community dataset for large-sample hydrology, *Sci Data*, 10, 61, <https://doi.org/10.1038/s41597-023-01975-w>, publisher: Nature Publishing Group, 2023.
- Laaha, G. and Koffler, D.: Ifstat: Calculation of Low Flow Statistics for Daily Stream Flow Data. R package version 0.9.12, 2022.
- 790 Lee, S. and Ajami, H.: Comprehensive assessment of baseflow responses to long-term meteorological droughts across the United States, *Journal of Hydrology*, 626, 130 256, <https://doi.org/10.1016/j.jhydrol.2023.130256>, 2023.
- Lees, T., Reece, S., Kratzert, F., Klotz, D., Gauch, M., De Bruijn, J., Kumar Sahu, R., Greve, P., Slater, L., and Dadson, S. J.: Hydrological concept formation inside long short-term memory (LSTM) networks, *Hydrology and Earth System Sciences*, 26, 3079–3101, <https://doi.org/10.5194/hess-26-3079-2022>, publisher: Copernicus GmbH, 2022.
- 795 Mahto, S. S. and Mishra, V.: Global evidence of rapid flash drought recovery by extreme precipitation, *Environ. Res. Lett.*, 19, 044 031, <https://doi.org/10.1088/1748-9326/ad300c>, publisher: IOP Publishing, 2024.
- Marty, C., Michel, A., Jonas, T., Steijn, C., Muelchi, R., and Kotlarski, S.: SPASS – new gridded climatological snow datasets for Switzerland: Potential and limitations, *EGUsphere*, pp. 1–21, <https://doi.org/10.5194/egusphere-2025-413>, publisher: Copernicus GmbH, 2025.
- 800 Massari, C., Avanzi, F., Bruno, G., Gabellani, S., Penna, D., and Camici, S.: Evaporation enhancement drives the European water-budget deficit during multi-year droughts, *Hydrology and Earth System Sciences*, 26, 1527–1543, <https://doi.org/10.5194/hess-26-1527-2022>, publisher: Copernicus GmbH, 2022.



- Matanó, A., Berghuijs, W. R., Mazzoleni, M., Ruiter, M. C. d., Ward, P. J., and Loon, A. F. V.: Compound and consecutive drought-flood events at a global scale, *Environ. Res. Lett.*, 19, 064 048, <https://doi.org/10.1088/1748-9326/ad4b46>, publisher: IOP Publishing, 2024.
- 805 McKee, T., Doesken, N., and Kleist, J.: THE RELATIONSHIP OF DROUGHT FREQUENCY AND DURATION TO TIME SCALES, Eight conference on applied climatology, 17-22 January 1993, Anaheim, California, <https://www.semanticscholar.org/paper/THE-RELATIONSHIP-OF-DROUGHT-FREQUENCY-AND-DURATION-McKee-Doesken/c3f7136d6cb726b295eb34565a8270177c57f40f>, 1993.
- Melsen, L. A. and Guse, B.: Hydrological Drought Simulations: How Climate and Model Structure Control Parameter Sensitivity, *Water Resources Research*, 55, 10 527–10 547, <https://doi.org/10.1029/2019WR025230>, <https://onlinelibrary.wiley.com/doi/pdf/10.1029/2019WR025230>, 2019.
- 810 MeteoSwiss: Daily Precipitation (final analysis): RhiresD, https://www.meteoswiss.admin.ch/dam/jcr:4f51f0f1-0fe3-48b5-9de0-15666327e63c/ProdDoc_RhiresD.pdf, 2021a.
- MeteoSwiss: Daily Mean, Minimum and Maximum Temperature: TabsD, TminD, TmaxD, https://www.meteoswiss.admin.ch/dam/jcr:818a4d17-cb0c-4e8b-92c6-1a1bdf5348b7/ProdDoc_TabsD.pdf, 2021b.
- 815 MeteoSwiss: Daily Relative Sunshine Duration: SrelD, https://www.meteoschweiz.admin.ch/dam/jcr:981891db-30d1-47cc-a2e1-50c270bdaf22/ProdDoc_SrelD.pdf, 2021c.
- MeteoSwiss: Spatial Climate Analyses - MeteoSwiss, <https://www.meteoswiss.admin.ch/climate/the-climate-of-switzerland/spatial-climate-analyses.html>, 2024.
- 820 MeteoSwiss: Open Data - MeteoSchweiz, <https://www.meteoschweiz.admin.ch/service-und-publikationen/service/open-data.html>, 2025.
- Michel, A., Aschauer, J., Jonas, T., Gubler, S., Kotlarski, S., and Marty, C.: SnowQM 1.0: A fast R Package for bias-correcting spatial fields of snow water equivalent using quantile mapping, *Geoscientific Model Development Discussions*, pp. 1–28, <https://doi.org/10.5194/gmd-2022-298>, publisher: Copernicus GmbH, 2023.
- Mishra, A. K. and Singh, V. P.: A review of drought concepts, *Journal of Hydrology*, 391, 202–216, <https://doi.org/10.1016/j.jhydrol.2010.07.012>, 2010.
- 825 Mott, R.: Climatological snow data since 1998, OSHD. *EnviDat*. <https://www.doi.org/10.16904/envidat.401>, 2023.
- Mott, R., Winstral, A., Cluzet, B., Helbig, N., Magnusson, J., Mazzotti, G., Quéno, L., Schirmer, M., Webster, C., and Jonas, T.: Operational snow-hydrological modeling for Switzerland, *Front. Earth Sci.*, 11, <https://doi.org/10.3389/feart.2023.1228158>, publisher: Frontiers, 2023.
- Muelchi, R., Rössler, O., Schwanbeck, J., Weingartner, R., and Martius, O.: River runoff in Switzerland in a changing climate – changes in moderate extremes and their seasonality, *Hydrology and Earth System Sciences*, 25, 3577–3594, <https://doi.org/10.5194/hess-25-3577-2021>, publisher: Copernicus GmbH, 2021a.
- 830 Muelchi, R., Rössler, O., Schwanbeck, J., Weingartner, R., and Martius, O.: River runoff in Switzerland in a changing climate – runoff regime changes and their time of emergence, *Hydrology and Earth System Sciences*, 25, 3071–3086, <https://doi.org/10.5194/hess-25-3071-2021>, publisher: Copernicus GmbH, 2021b.
- 835 Muñoz-Sabater, J., Dutra, E., Agustí-Panareda, A., Albergel, C., Arduini, G., Balsamo, G., Boussetta, S., Choulga, M., Harrigan, S., Hersbach, H., Martens, B., Miralles, D. G., Piles, M., Rodríguez-Fernández, N. J., Zsoter, E., Buontempo, C., and Thépaut, J.-N.: ERA5-Land: a state-of-the-art global reanalysis dataset for land applications, *Earth System Science Data*, 13, 4349–4383, <https://doi.org/10.5194/essd-13-4349-2021>, publisher: Copernicus GmbH, 2021.



- Myronidis, D., Fotakis, D., Ioannou, K., and Sgouropoulou, K.: Comparison of ten notable meteorological drought indices on tracking
 840 the effect of drought on streamflow, *Hydrological Sciences Journal*, 63, 2005–2019, <https://doi.org/10.1080/02626667.2018.1554285>, publisher: Taylor & Francis _eprint: <https://doi.org/10.1080/02626667.2018.1554285>, 2018.
- Nathan, R. J. and McMahon, T. A.: Evaluation of automated techniques for base flow and recession analyses, *Water Resources Research*, 26, 1465–1473, <https://doi.org/10.1029/WR026i007p01465>, _eprint: <https://onlinelibrary.wiley.com/doi/pdf/10.1029/WR026i007p01465>, 1990.
- 845 Naumann, G., Cammalleri, C., Mentaschi, L., and Feyen, L.: Increased economic drought impacts in Europe with anthropogenic warming, *Nat. Clim. Chang.*, 11, 485–491, <https://doi.org/10.1038/s41558-021-01044-3>, number: 6 Publisher: Nature Publishing Group, 2021.
- Orth, R. and Destouni, G.: Drought reduces blue-water fluxes more strongly than green-water fluxes in Europe, *Nat Commun*, 9, 3602, <https://doi.org/10.1038/s41467-018-06013-7>, 2018.
- Otero, N., Horton, P., Martius, O., Allen, S., Zappa, M., Wechsler, T., and Schaeffli, B.: Impacts of hot-dry conditions on hydropower
 850 production in Switzerland, *Environ. Res. Lett.*, 18, 064 038, <https://doi.org/10.1088/1748-9326/acd8d7>, publisher: IOP Publishing, 2023.
- Parry, S., Prudhomme, C., Wilby, R. L., and Wood, P. J.: Drought termination: Concept and characterisation, *Progress in Physical Geography: Earth and Environment*, 40, 743–767, <https://doi.org/10.1177/0309133316652801>, publisher: SAGE Publications Ltd, 2016.
- Parry, S., Wilby, R., Prudhomme, C., Wood, P., and McKenzie, A.: Demonstrating the utility of a drought termination framework: prospects for groundwater level recovery in England and Wales in 2018 or beyond, *Environ. Res. Lett.*, 13, 064 040, [https://doi.org/10.1088/1748-](https://doi.org/10.1088/1748-9326/aac78c)
 855 [9326/aac78c](https://doi.org/10.1088/1748-9326/aac78c), publisher: IOP Publishing, 2018.
- Pebesma, E.: Simple Features for R: Standardized Support for Spatial Vector Data, *The R Journal*, 10, 439–446, <https://journal.r-project.org/archive/2018/RJ-2018-009/index.html>, 2018.
- Pebesma, E. and Bivand, R.: *Spatial Data Science: With Applications in R*, Chapman and Hall/CRC, New York, <https://doi.org/10.1201/9780429459016>, 2023.
- 860 Peña-Angulo, D., Vicente-Serrano, S. M., Domínguez-Castro, F., Lorenzo-Lacruz, J., Murphy, C., Hannaford, J., Allan, R. P., Tramblay, Y., Reig-Gracia, F., and El Kenawy, A.: The Complex and Spatially Diverse Patterns of Hydrological Droughts Across Europe, *Water Resources Research*, 58, e2022WR031 976, <https://doi.org/10.1029/2022WR031976>, _eprint: <https://onlinelibrary.wiley.com/doi/pdf/10.1029/2022WR031976>, 2022.
- Peña-Gallardo, M., Vicente-Serrano, S. M., Hannaford, J., Lorenzo-Lacruz, J., Svoboda, M., Domínguez-Castro, F., Maneta, M., Tomas-
 865 Burguera, M., and Kenawy, A. E.: Complex influences of meteorological drought time-scales on hydrological droughts in natural basins of the contiguous Unites States, *Journal of Hydrology*, 568, 611–625, <https://doi.org/10.1016/j.jhydrol.2018.11.026>, 2019.
- Poussin, C., Massot, A., Ginzler, C., Weber, D., Chatenoux, B., Lacroix, P., Piller, T., Nguyen, L., and Giuliani, G.: Drying conditions in Switzerland – indication from a 35-year Landsat time-series analysis of vegetation water content estimates to support SDGs, *Big Earth Data*, 5, 445–475, <https://doi.org/10.1080/20964471.2021.1974681>, publisher: Taylor & Francis _eprint: <https://doi.org/10.1080/20964471.2021.1974681>, 2021.
 870
- Qiu, J., Shen, Z., Leng, G., and Wei, G.: Synergistic effect of drought and rainfall events of different patterns on watershed systems, *Sci Rep*, 11, 18 957, <https://doi.org/10.1038/s41598-021-97574-z>, number: 1 Publisher: Nature Publishing Group, 2021.
- Ranasinghe, R., Ruane, A. C., Vautard, R., Arnell, N., Coppola, E., Cruz, F. A., Dessai, S., Islam, A. S., Rahimi, M., Ruiz Carrascal, D., Sillmann, J., Sylla, M. B., Tebaldi, C., Wang, W., and Zaaboul, R.: Climate Change Information for Regional Impact and for Risk
 875 Assessment., in: *Climate Change 2021: The Physical Science Basis. Contribution of Working Group I to the Sixth Assessment Report*



- of the Intergovernmental Panel on Climate Change., pp. 1767–1926, Cambridge University Press, Cambridge, United Kingdom and New York, NY, USA, doi:10.1017/9781009157896.014, 2021.
- Rangecroft, S., Van Loon, A. F., Maureira, H., Verbist, K., and Hannah, D. M.: An observation-based method to quantify the human influence on hydrological drought: upstream–downstream comparison, *Hydrological Sciences Journal*, 64, 276–287, <https://doi.org/10.1080/02626667.2019.1581365>, 2019.
- Raposo, V. d. M. B., Costa, V. A. F., and Rodrigues, A. F.: A review of recent developments on drought characterization, propagation, and influential factors, *Science of The Total Environment*, 898, 165 550, <https://doi.org/10.1016/j.scitotenv.2023.165550>, 2023.
- Samaniego, L., Kumar, R., and Zink, M.: Implications of Parameter Uncertainty on Soil Moisture Drought Analysis in Germany, *Journal of Hydrometeorology*, 14, 47–68, <https://doi.org/10.1175/JHM-D-12-075.1>, publisher: American Meteorological Society Section: Journal of Hydrometeorology, 2013.
- Samaniego, L., Thober, S., Kumar, R., Wanders, N., Rakovec, O., Pan, M., Zink, M., Sheffield, J., Wood, E. F., and Marx, A.: Anthropogenic warming exacerbates European soil moisture droughts, *Nature Clim Change*, 8, 421–426, <https://doi.org/10.1038/s41558-018-0138-5>, number: 5 Publisher: Nature Publishing Group, 2018.
- Sarailidis, G., Vasiliades, L., and Loukas, A.: Analysis of streamflow droughts using fixed and variable thresholds, *Hydrological Processes*, 33, 414–431, <https://doi.org/10.1002/hyp.13336>, _eprint: <https://onlinelibrary.wiley.com/doi/pdf/10.1002/hyp.13336>, 2019.
- Savelli, E., Rusca, M., Cloke, H., and Di Baldassarre, G.: Drought and society: Scientific progress, blind spots, and future prospects, *WIREs Climate Change*, 13, e761, <https://doi.org/10.1002/wcc.761>, _eprint: <https://onlinelibrary.wiley.com/doi/pdf/10.1002/wcc.761>, 2022.
- Scherrer, S. C., Hirschi, M., Spirig, C., Maurer, F., and Kotlarski, S.: Trends and drivers of recent summer drying in Switzerland, *Environ. Res. Commun.*, <https://doi.org/10.1088/2515-7620/ac4fb9>, 2022.
- Scherrer, S. C., Göldi, M., Gubler, S., Steger, C. R., and Kotlarski, S.: Towards a spatial snow climatology for Switzerland: Comparison and validation of existing datasets, *Meteorologische Zeitschrift*, <https://doi.org/10.1127/metz/2023/1210>, publisher: Schweizerbart'sche Verlagsbuchhandlung, 2023.
- Schürch, M., Kozel, R., and Jemelin, L.: Hydrogeological mapping in Switzerland, *Hydrogeol J*, 15, 799–808, <https://doi.org/10.1007/s10040-006-0136-y>, 2007.
- Shapiro, S. S. and Wilk, M. B.: An Analysis of Variance Test for Normality (Complete Samples), *Biometrika*, 52, 591–611, <https://doi.org/10.2307/2333709>, publisher: [Oxford University Press, Biometrika Trust], 1965.
- Sideris, I. V., Gabella, M., Erdin, R., and Germann, U.: Real-time radar–rain–gauge merging using spatio-temporal co-kriging with external drift in the alpine terrain of Switzerland, *Quarterly Journal of the Royal Meteorological Society*, 140, 1097–1111, <https://doi.org/10.1002/qj.2188>, _eprint: <https://onlinelibrary.wiley.com/doi/pdf/10.1002/qj.2188>, 2014.
- Stagge, J. H., Tallaksen, L. M., Gudmundsson, L., Van Loon, A. F., and Stahl, K.: Candidate Distributions for Climatological Drought Indices (SPI and SPEI), *International Journal of Climatology*, 35, 4027–4040, <https://doi.org/10.1002/joc.4267>, _eprint: <https://onlinelibrary.wiley.com/doi/pdf/10.1002/joc.4267>, 2015.
- Staudinger, M., Stahl, K., and Seibert, J.: A drought index accounting for snow, *Water Resources Research*, 50, 7861–7872, <https://doi.org/10.1002/2013WR015143>, _eprint: <https://onlinelibrary.wiley.com/doi/pdf/10.1002/2013WR015143>, 2014.
- Staudinger, M., Stoelzle, M., Seeger, S., Seibert, J., Weiler, M., and Stahl, K.: Catchment water storage variation with elevation, *Hydrological Processes*, 31, 2000–2015, <https://doi.org/10.1002/hyp.11158>, _eprint: <https://onlinelibrary.wiley.com/doi/pdf/10.1002/hyp.11158>, 2017.
- Stocker, B. D.: cwd v1.0: R package for cumulative water deficit calculation (v1.0). Zenodo. <https://doi.org/10.5281/zenodo.5359053>, 2021.



- Stocker, B. D., Tumber-Dávila, S. J., Konings, A. G., Anderson, M. C., Hain, C., and Jackson, R. B.: Global patterns of water storage in the rooting zones of vegetation, *Nat. Geosci.*, 16, 250–256, <https://doi.org/10.1038/s41561-023-01125-2>, number: 3 Publisher: Nature Publishing Group, 2023.
- 915 Stoele, M., Schuetz, T., Weiler, M., Stahl, K., and Tallaksen, L. M.: Beyond binary baseflow separation: a delayed-flow index for multiple streamflow contributions, *Hydrology and Earth System Sciences*, 24, 849–867, <https://doi.org/10.5194/hess-24-849-2020>, publisher: Copernicus GmbH, 2020.
- Streeb, N., Lustenberger, F., and Zappa, M.: Beurteilung der Beeinflussung des Abflusses an NAWA-Messstellen. Detailbericht des BAFU-Projekts HydCheck., Tech. rep., Eidg. Forschungsanstalt WSL, Birmensdorf, https://www.bafu.admin.ch/dam/bafu/de/dokumente/wasser/externe-studien-berichte/beurteilung-der-beeinflussung-des-abflusses-an-nawa-messstellen.pdf.download.pdf/20241007_HydCheck_Detailbericht.pdf, 2024.
- 920 Sur, C., Park, S.-Y., Kim, J.-S., and Lee, J.-H.: Prognostic and diagnostic assessment of hydrological drought using water and energy budget-based indices, *Journal of Hydrology*, 591, 125 549, <https://doi.org/10.1016/j.jhydrol.2020.125549>, 2020.
- 925 Sutanto, S. J. and Van Lanen, H. A. J.: Catchment memory explains hydrological drought forecast performance, *Sci Rep*, 12, 2689, <https://doi.org/10.1038/s41598-022-06553-5>, number: 1 Publisher: Nature Publishing Group, 2022.
- Swiss Confederation: Nationale Trockenheitsplattform, <https://www.trockenheit.admin.ch/de>, 2025.
- Swisstopo: Bodeneignungskarte der Schweiz, <https://www.bfs.admin.ch/bfs/de/home/dienstleistungen/geostat/geodaten-bundesstatistik/boden-nutzung-bedeckung-eignung/abgeleitete-und-andere-daten/bodeneignungskarte-schweiz.html>, 2020.
- 930 Swisstopo: swissALTI3D - Das hoch aufgelöste Terrainmodell der Schweiz, <https://backend.swisstopo.admin.ch/fileservice/sdweb-docs-prod-swisstopoch-files/files/2023/11/14/6d40e558-c3df-483a-bd88-99ab93b88f16.pdf>, 2022.
- Tallaksen, L. M. and Van Lanen, H. A. J., eds.: Hydrological drought: processes and estimation methods for streamflow and groundwater, no. 48 in *Developments in Water Science*, Elsevier Science B.V., Amsterdam, the Netherlands, 2004.
- Tallaksen, L. M., Madsen, H., and Clausen, B.: On the definition and modelling of streamflow drought duration and deficit volume, *Hydrological Sciences Journal*, 42, 15–33, <https://doi.org/10.1080/02626669709492003>, publisher: Taylor & Francis _eprint: <https://doi.org/10.1080/02626669709492003>, 1997.
- 935 Tarasova, L., Gnann, S., Yang, S., Hartmann, A., and Wagener, T.: Catchment characterization: Current descriptors, knowledge gaps and future opportunities, *Earth-Science Reviews*, 252, 104 739, <https://doi.org/10.1016/j.earscirev.2024.104739>, 2024.
- Tijdeman, E., Barker, L. J., Svoboda, M. D., and Stahl, K.: Natural and Human Influences on the Link Between Meteorological and Hydrological Drought Indices for a Large Set of Catchments in the Contiguous United States, *Water Resources Research*, 54, 6005–6023, <https://doi.org/10.1029/2017WR022412>, _eprint: <https://onlinelibrary.wiley.com/doi/pdf/10.1029/2017WR022412>, 2018.
- 940 Tijdeman, E., Stahl, K., and Tallaksen, L. M.: Drought Characteristics Derived Based on the Standardized Streamflow Index: A Large Sample Comparison for Parametric and Nonparametric Methods, *Water Resources Research*, 56, e2019WR026315, <https://doi.org/10.1029/2019WR026315>, _eprint: <https://onlinelibrary.wiley.com/doi/pdf/10.1029/2019WR026315>, 2020.
- 945 Tijdeman, E., Blauhut, V., Stoele, M., Menzel, L., and Stahl, K.: Different drought types and the spatial variability in their hazard, impact, and propagation characteristics, *Natural Hazards and Earth System Sciences*, 22, 2099–2116, <https://doi.org/10.5194/nhess-22-2099-2022>, publisher: Copernicus GmbH, 2022.
- Tripathy, K. P. and Mishra, A. K.: How Unusual Is the 2022 European Compound Drought and Heat-wave Event?, *Geophysical Research Letters*, 50, e2023GL105453, <https://doi.org/10.1029/2023GL105453>, _eprint: <https://onlinelibrary.wiley.com/doi/pdf/10.1029/2023GL105453>, 2023.
- 950



- Tschurr, F., Feigenwinter, I., Fischer, A. M., and Kotlarski, S.: Climate Scenarios and Agricultural Indices: A Case Study for Switzerland, *Atmosphere*, 11, 535, <https://doi.org/10.3390/atmos11050535>, number: 5 Publisher: Multidisciplinary Digital Publishing Institute, 2020.
- USGS: Drainage Density | U.S. Geological Survey, <https://www.usgs.gov/media/images/drainage-density>, 2023.
- Van Lanen, H. a. J., Wanders, N., Tallaksen, L. M., and Van Loon, A. F.: Hydrological drought across the world: impact of climate and physical catchment structure, *Hydrology and Earth System Sciences*, 17, 1715–1732, <https://doi.org/10.5194/hess-17-1715-2013>, publisher: Copernicus GmbH, 2013.
- Van Loon, A. F.: Hydrological drought explained, *WIREs Water*, 2, 359–392, <https://doi.org/10.1002/wat2.1085>, eprint: <https://onlinelibrary.wiley.com/doi/pdf/10.1002/wat2.1085>, 2015.
- Van Loon, A. F. and Laaha, G.: Hydrological drought severity explained by climate and catchment characteristics, *Journal of Hydrology*, 526, 3–14, <https://doi.org/10.1016/j.jhydrol.2014.10.059>, 2015.
- Van Loon, A. F. and Van Lanen, H. a. J.: A process-based typology of hydrological drought, *Hydrology and Earth System Sciences*, 16, 1915–1946, <https://doi.org/10.5194/hess-16-1915-2012>, publisher: Copernicus GmbH, 2012.
- Van Loon, A. F., Rangelcroft, S., Coxon, G., Breña Naranjo, J. A., Van Ogtrop, F., and Van Lanen, H. A. J.: Using paired catchments to quantify the human influence on hydrological droughts, *Hydrology and Earth System Sciences*, 23, 1725–1739, <https://doi.org/10.5194/hess-23-1725-2019>, publisher: Copernicus GmbH, 2019.
- Vicente-Serrano, S. M., Beguería, S., and López-Moreno, J. I.: A Multiscalar Drought Index Sensitive to Global Warming: The Standardized Precipitation Evapotranspiration Index, *Journal of Climate*, 23, 1696–1718, <https://doi.org/10.1175/2009JCLI2909.1>, publisher: American Meteorological Society Section: Journal of Climate, 2010.
- Vicente-Serrano, S. M., Peña-Angulo, D., Beguería, S., Domínguez-Castro, F., Tomás-Burguera, M., Noguera, I., Gimeno-Sotelo, L., and El Kenawy, A.: Global drought trends and future projections, *Philosophical Transactions of the Royal Society A: Mathematical, Physical and Engineering Sciences*, 380, 20210285, <https://doi.org/10.1098/rsta.2021.0285>, publisher: Royal Society, 2022.
- Viviroli, D., Zappa, M., Gurtz, J., and Weingartner, R.: An introduction to the hydrological modelling system PREVAH and its pre- and post-processing-tools, *Environmental Modelling & Software*, 24, 1209–1222, <https://doi.org/10.1016/j.envsoft.2009.04.001>, 2009.
- von Matt, C. N., Muelchi, R., Gudmundsson, L., and Martius, O.: Compound droughts under climate change in Switzerland, *Natural Hazards and Earth System Sciences*, 24, 1975–2001, <https://doi.org/10.5194/nhess-24-1975-2024>, publisher: Copernicus GmbH, 2024.
- von Matt, C. N., Martius, O., and Stocker, B. D.: HYD-RESPONSES: High-resolution daily catchment-level time series for relevant hydro-meteorological variables, (water) deficit accumulation and streamflow droughts for Switzerland, <https://doi.org/10.5281/zenodo.14713275>, 2025.
- Weingartner, R. and Schwanbeck, J.: Veränderung der Niedrigwasserabflüsse und der kleinsten saisonalen Abflüsse in der Schweiz im Zeitraum 1961 – 2018. Im Auftrag des Bundesamts für Umwelt (BAFU), Bern, Schweiz, 41 S., Tech. rep., Bern, Schweiz, 2020.
- Wickham, H., Averick, M., Bryan, J., Chang, W., McGowan, L. D., François, R., Golemund, G., Hayes, A., Henry, L., Hester, J., Kuhn, M., Pedersen, T. L., Miller, E., Bache, S. M., Müller, K., Ooms, J., Robinson, D., Seidel, D. P., Spinu, V., Takahashi, K., Vaughan, D., Wilke, C., Woo, K., and Yutani, H.: Welcome to the Tidyverse, *Journal of Open Source Software*, 4, 1686, <https://doi.org/10.21105/joss.01686>, 2019.
- WMO and GWP: Handbook of Drought Indicators and Indices (M. Svoboda and B. A. Fuchs). Integrated Drought Management Programme (IDMP), Integrated Drought Management Tools and Guidelines Series 2. Geneva., 2016.



- Wu, J., Chen, X., Love, C. A., Yao, H., Chen, X., and AghaKouchak, A.: Determination of water required to recover from hydrological drought: Perspective from drought propagation and non-standardized indices, *Journal of Hydrology*, 590, 125 227, <https://doi.org/10.1016/j.jhydrol.2020.125227>, 2020.
- 990 Wu, J., Chen, X., Yuan, X., Yao, H., Zhao, Y., and AghaKouchak, A.: The interactions between hydrological drought evolution and precipitation-streamflow relationship, *Journal of Hydrology*, 597, 126 210, <https://doi.org/10.1016/j.jhydrol.2021.126210>, 2021.
- Wu, J., Mallakpour, I., Yuan, X., Yao, H., Wang, G., and Chen, X.: Impact of the false intensification and recovery on the hydrological drought internal propagation, *Weather and Climate Extremes*, 36, 100 430, <https://doi.org/10.1016/j.wace.2022.100430>, 2022.
- Xu, Z., Wu, Z., Guo, X., and He, H.: Estimation of water required to recover from agricultural drought: Perspective from regression and probabilistic analysis methods, *Journal of Hydrology*, 617, 128 888, <https://doi.org/10.1016/j.jhydrol.2022.128888>, 2023.
- 995 Yihdego, Y., Vaheddoost, B., and Al-Weshah, R. A.: Drought indices and indicators revisited, *Arab J Geosci*, 12, 69, <https://doi.org/10.1007/s12517-019-4237-z>, 2019.
- Zambrano-Bigiarini, M.: hydroTSM: Time Series Management, Analysis and Interpolation for Hydrological ModellingR package version 0.6-0. URL <https://github.com/hzambran/hydroTSM>. DOI:10.5281/zenodo.839864., 2020.
- 1000 Zhou, Z., Shi, H., Fu, Q., Ding, Y., Li, T., and Liu, S.: Investigating the Propagation From Meteorological to Hydrological Drought by Introducing the Nonlinear Dependence With Directed Information Transfer Index, *Water Resources Research*, 57, e2021WR030 028, <https://doi.org/10.1029/2021WR030028>, _eprint: <https://onlinelibrary.wiley.com/doi/pdf/10.1029/2021WR030028>, 2021.

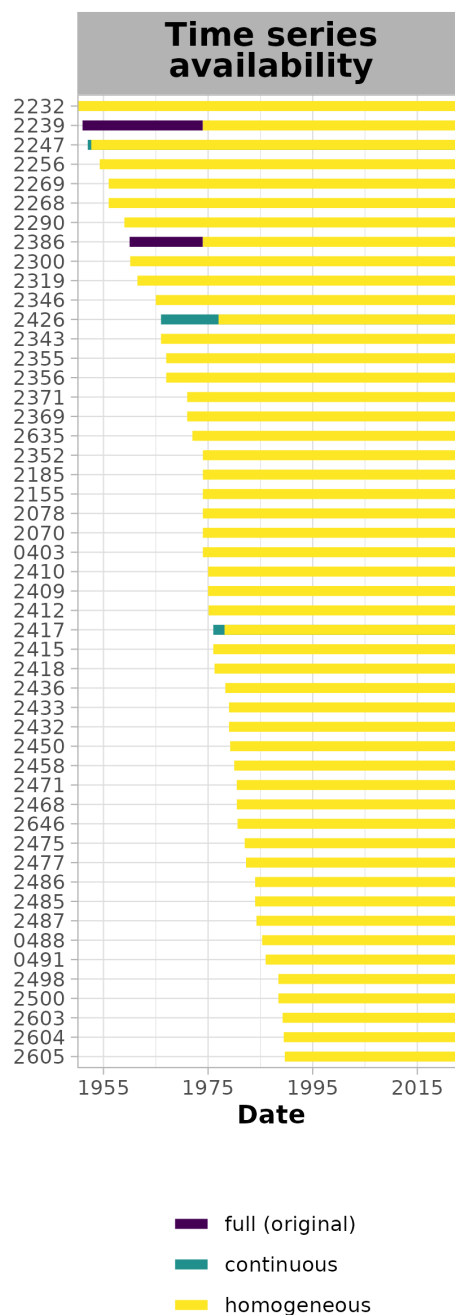


Figure 4. Streamflow time series availability for 50 example catchments. The colours indicate the periods covered by availability type. Complete is equivalent to the original time series provided by the FOEN. Continuous denotes the gap-checked time series and the homogeneous period accounts for homogeneity (starting at a breakpoint). In the case of overlapping periods, only the most important period type for analysis (e.g., homogeneous) is displayed. The importance of the periods for analysis is defined as follows: *homogeneous* is more important than *continuous* is more important than *full (original)*.

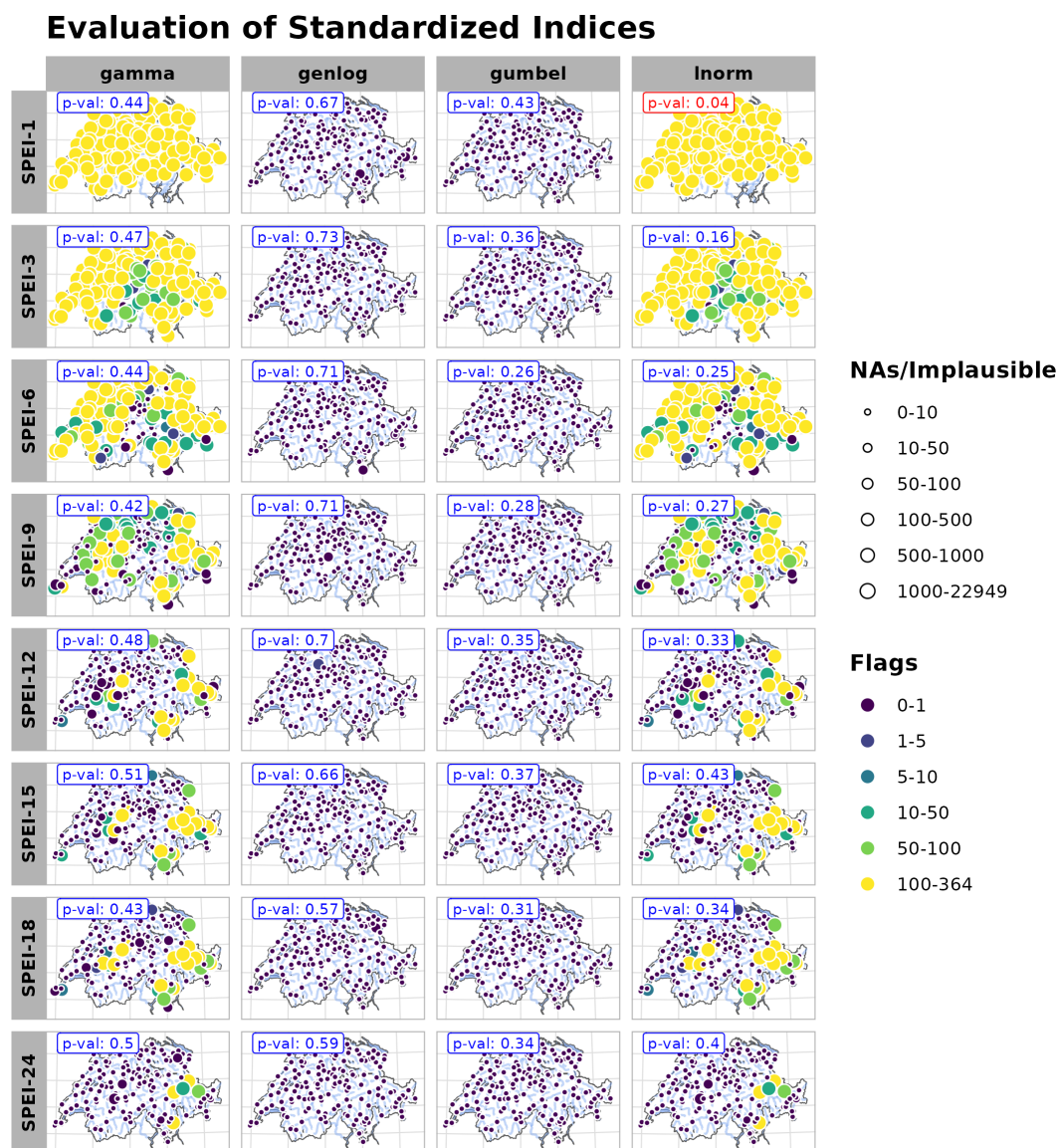


Figure 5. Evaluation statistics for the transformation of standardized (drought) indices. Information on the normality tests (p -values), flags and implausible/missing values for four example candidate distributions for the Standardized Precipitation and Evaporation Index (SPEI; Vicente-Serrano et al., 2010). The circle size indicates the number of missing and implausible values. Colours show the number of flags (= convergence issues) returned by the fitting function of the *SCI* R-package (Stagge et al., 2015; Gudmundsson and Stagge, 2016) for all days of the year (DOY). The maximum number of flags is equivalent to 366. Median p -values of the Shapiro-Wilk normality test (Shapiro and Wilk, 1965) were calculated by considering all catchments and are coloured in red in case of rejection ($p < 0.05$). The final HYD-RESPONSES dataset only provides SPEIs fitted by the *genlog*-distribution (best choice based on the evaluation criteria).

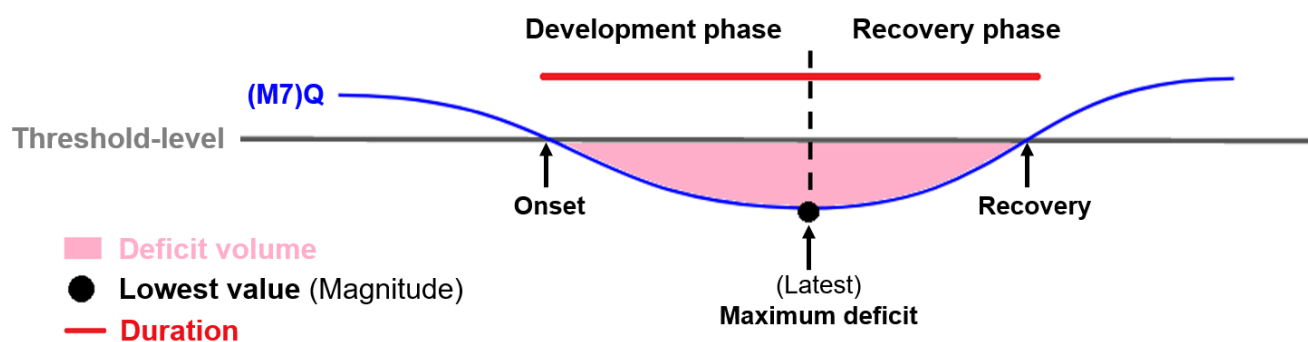


Figure 6. Schematic depiction of the event definition and phase subdivision. The extracted (streamflow) drought phases are characterized by duration, event start (onset), the latest date of the maximum streamflow deficit (anomaly), and event recovery. Additional characteristics are the drought intensity (deficit volume or accumulated deficit) and severity/magnitude (maximum streamflow deficit). The computation of other characteristics is left to the user.

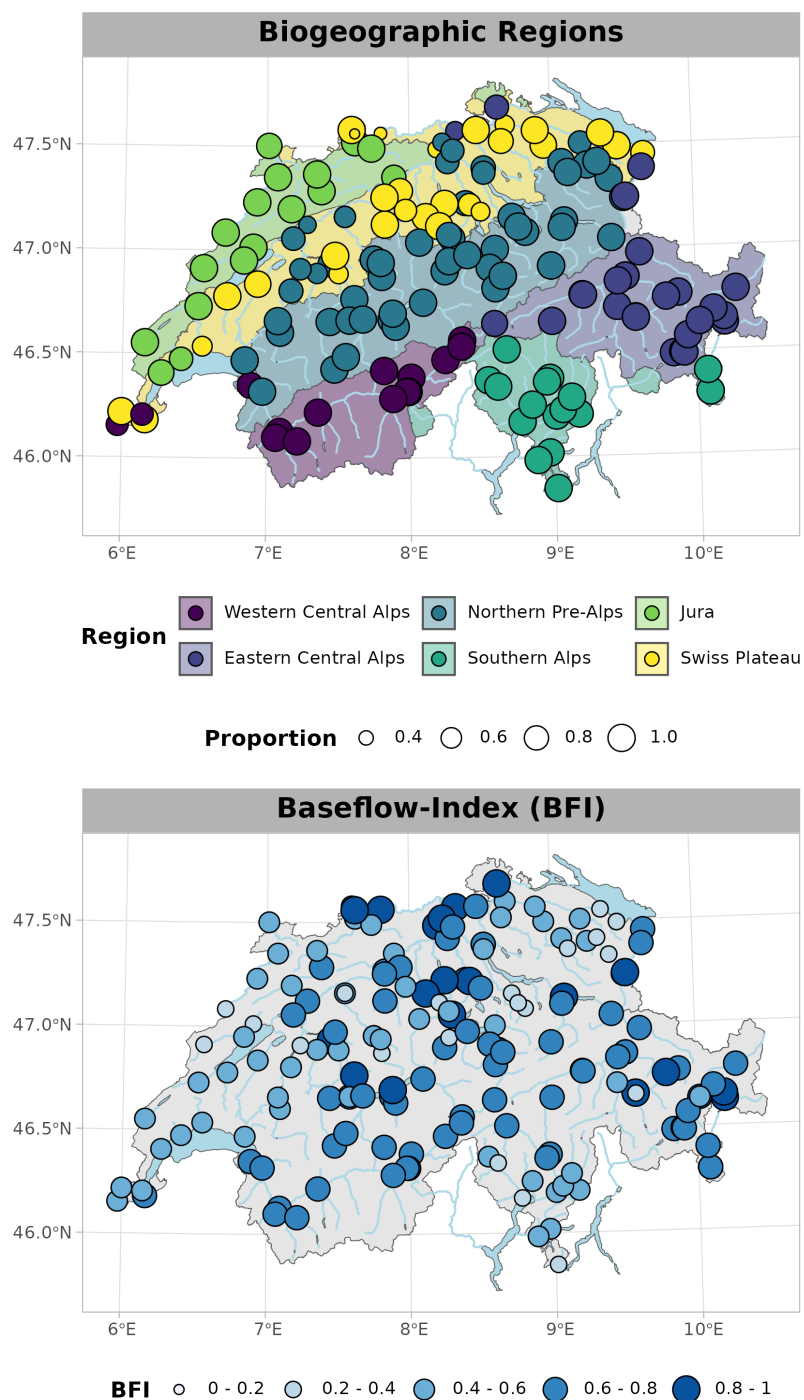


Figure 7. Catchment descriptors (examples). **Top:** Dominant (largest overlap percentage with the catchment area) biogeographic region (colours). Point sizes indicate the catchment area proportion covered by the dominant biogeographic region. **Bottom:** Baseflow-Index (BFI, Nathan and McMahon, 1990) for each catchment derived from the daily streamflow time series.

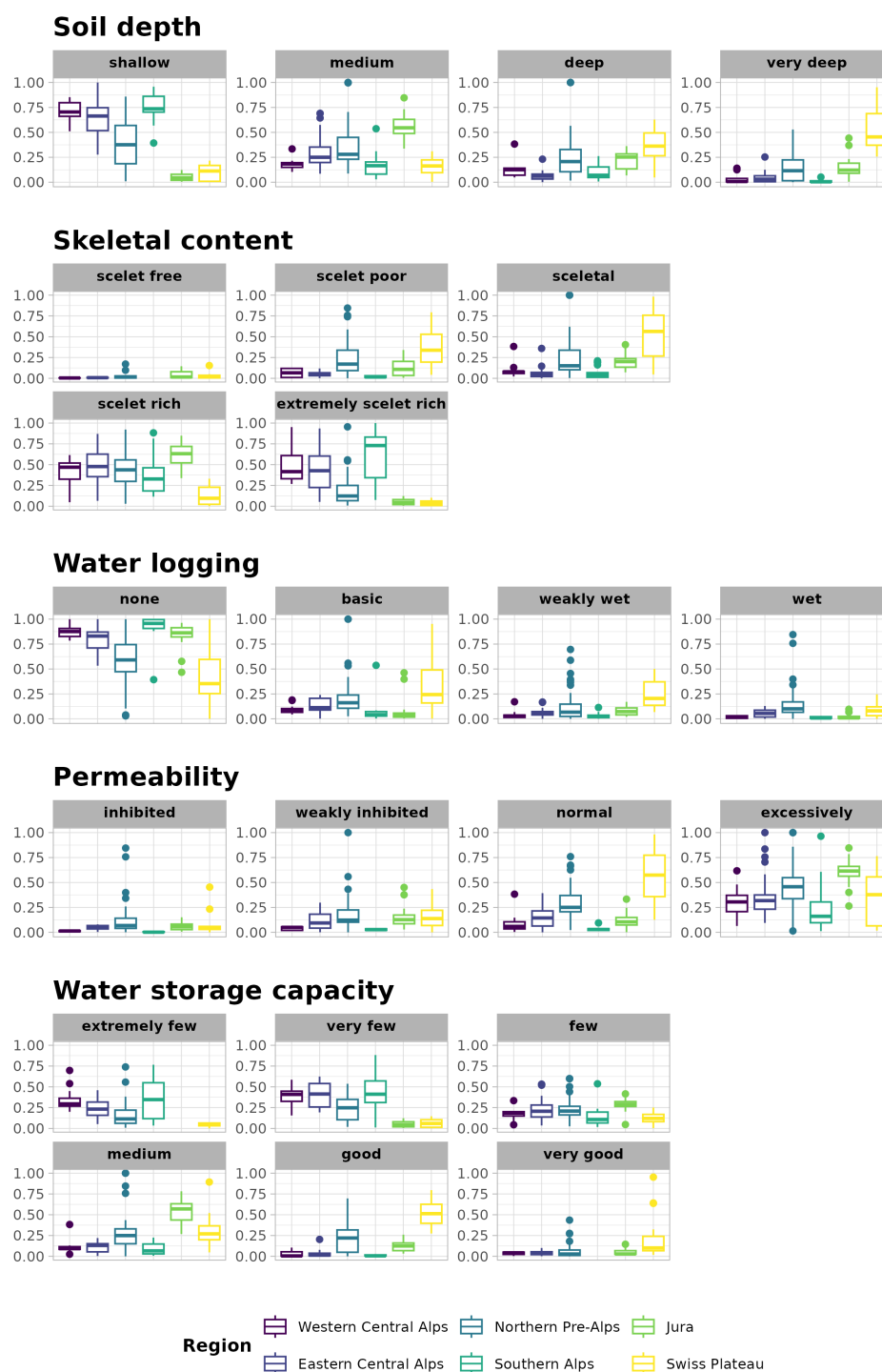


Figure 8. Catchment coverage fractions for all (sub-)categories of the soil characteristics: soil depth, skeletal content, water logging, soil permeability, and water storage capacity across regionalized catchment groups derived from the biogeographic regions of Switzerland (colours).



Drought 2022 - Example 2034 - Broye (Payerne, Caserne d'aviation)

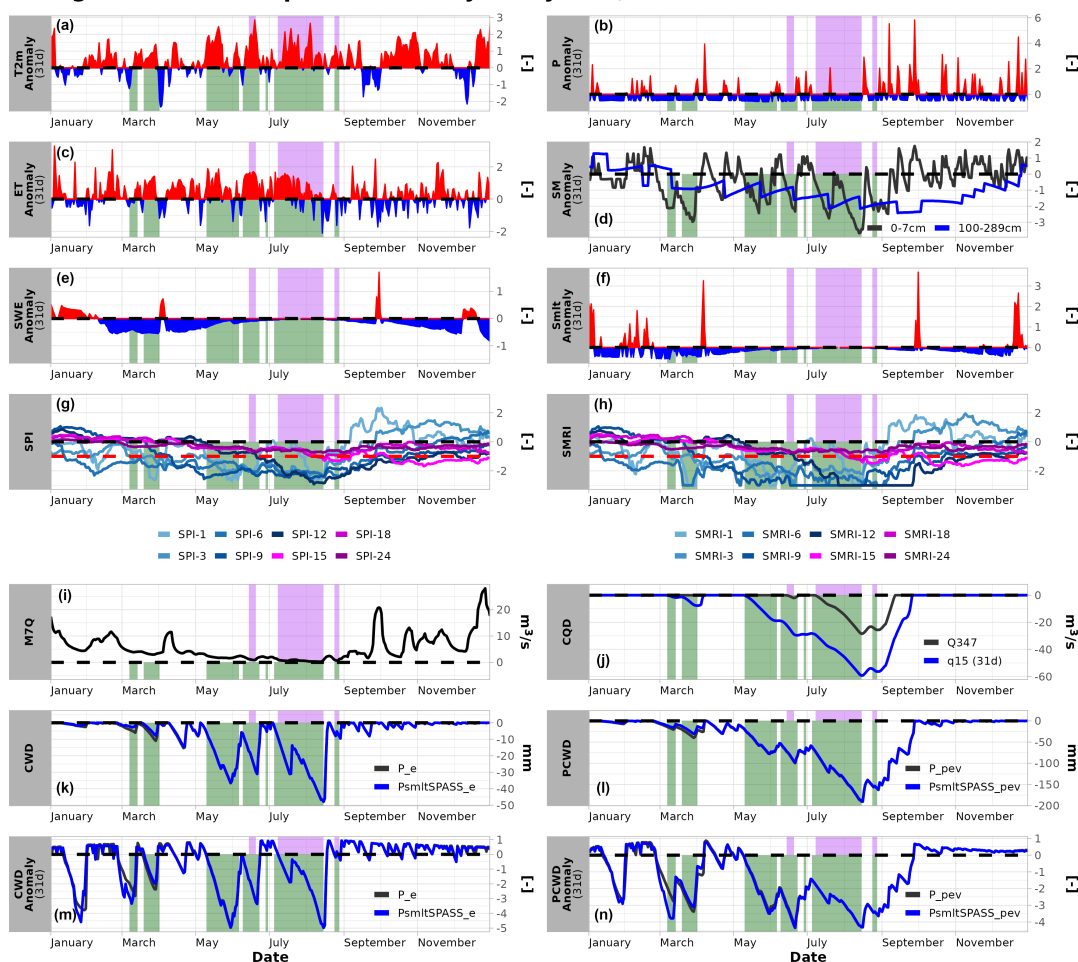


Figure 9. Hydro-meteorological time series for the Swiss Plateau catchment 2034 - Broye, Payerne (Caserne d'aviation) for the year 2022. Color shadings in all panels highlight drought periods based on two definitions: yearly Q347 (pink, fixed threshold approach) and a moving monthly 15th percentile threshold (green, variable threshold approach). (a) Moving monthly anomalies of the 2 m-temperature (T2m), positive anomalies are shown in red and negative anomalies in blue. (b) Moving monthly anomalies of the precipitation (P, RhiresD) (c) Moving monthly anomalies of the evaporation (ET, ERA5-land). (d) Moving monthly anomalies of the soil moisture volume (ESM ERA5-land), soil moisture anomalies are depicted for a near-surface SM-level (black, 0–7 cm) and the deepest level (blue, 100–289 cm) available from ERA5-Land. (e) Moving monthly anomalies of the snow water equivalent (SWE SPASS). (f) Moving monthly anomalies of the snowmelt (smlt, SPASS). (g) SPI colored by aggregation scales from 1- to 24-months. (h) SMRI colored by aggregation scales from 1- to 24-months. (i) Seven day average streamflow (M7Q). (j) The CQD time series shows the corresponding accumulated M7Q-deficits for both the fixed threshold approach (black) and the variable threshold approach (blue). (k) Absolute cumulative water deficit (CWD). (l) Potential cumulative water deficit (PCWD). (m) Monthly anomalies of the CWD (CWD anomaly). (n) Monthly anomalies of the PCWD. Time series of the cumulative water deficits for both absolute values and monthly anomalies are shown for both standard (black, P–E (P_e)) and snowmelt-corrected (blue, P–E+ Δ SWE ($P_{smltSPASS_e}$)) variants. The same is shown for cumulative potential water deficits which are based on the potential water balance (P–PET (P_{pev}) and P–PET+ Δ SWE ($P_{smltSPASS_pev}$)).



Median SPI-values during hydrological events

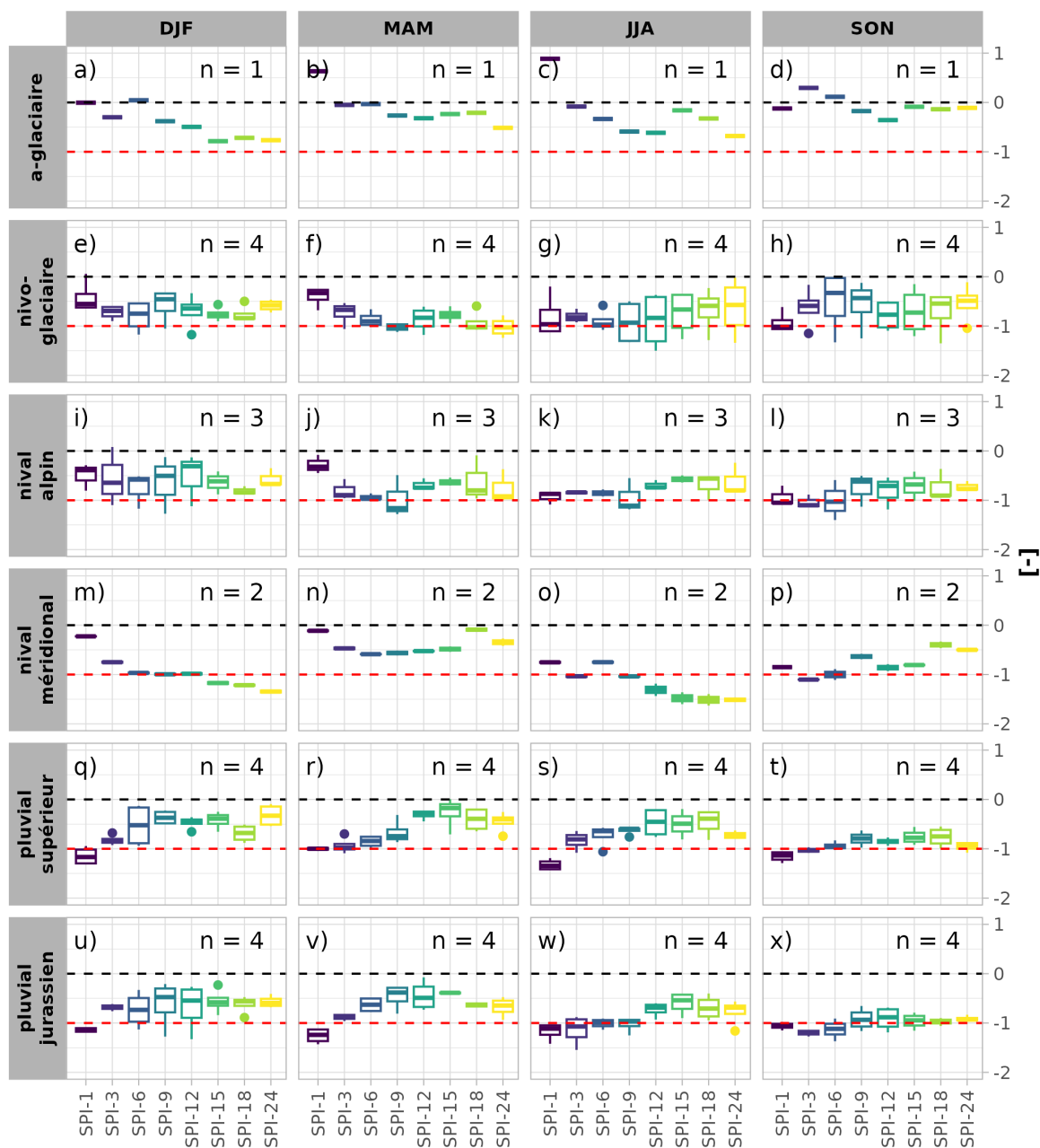


Figure 10. Median SPI values during hydrological drought conditions for all events of all catchments for six selected streamflow regime types across the four seasons winter (DJF), spring (MAM), summer (JJA) and autumn (SON). The streamflow regime types were selected to represent catchments with (dominant) glacial (a-glaciaire, nivo-glaciaire), snow (nival alpin, nival méridional) and pluvial processes (pluvial jurassien, pluvial supérieur) and spatial diversity. Hydrological drought events were defined by a moving monthly (31d) 15th-percentile (variable) threshold. Boxplots are coloured according to SPI aggregation time scales (1- to 24-months). Moderate drought conditions are indicated by the red dashed lines, the black dashed line indicates 0.

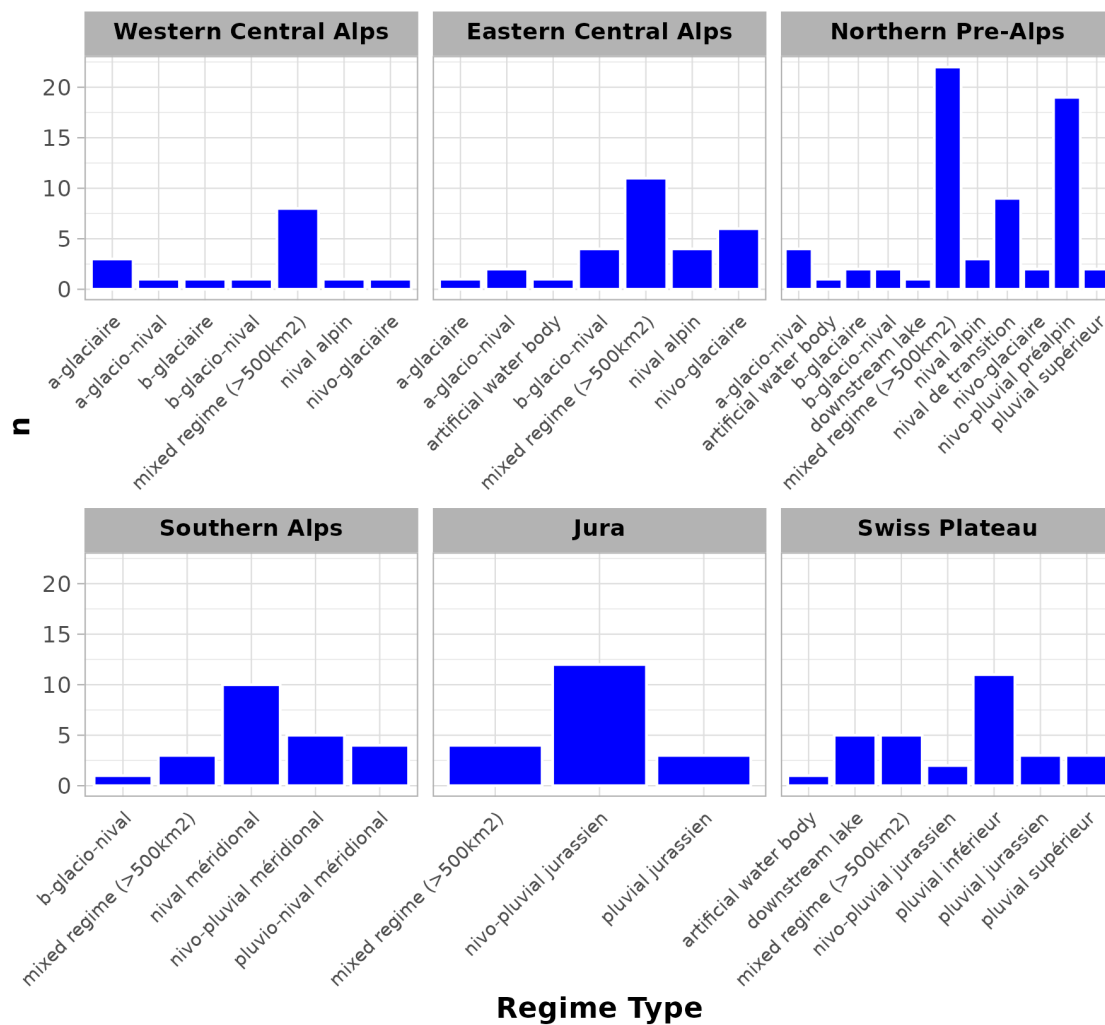


Figure A1. Streamflow regime type incidence among catchments grouped by the biogeographic regions of Switzerland (Western Central Alps, Eastern Central Alps, Northern Pre-Alps, Southern Alps, Jura and Swiss Plateau region; see Section 3.3 and also Fig. 7). The streamflow regime type classification was provided by the FOEN.